Assessing the Impact of Spatially Distributed Precipitation on Hydrological Modelling in Data-Scarce Mountainous Basin

Case Study: Rio Las Vacas

Muhammad Rifki Rasyid

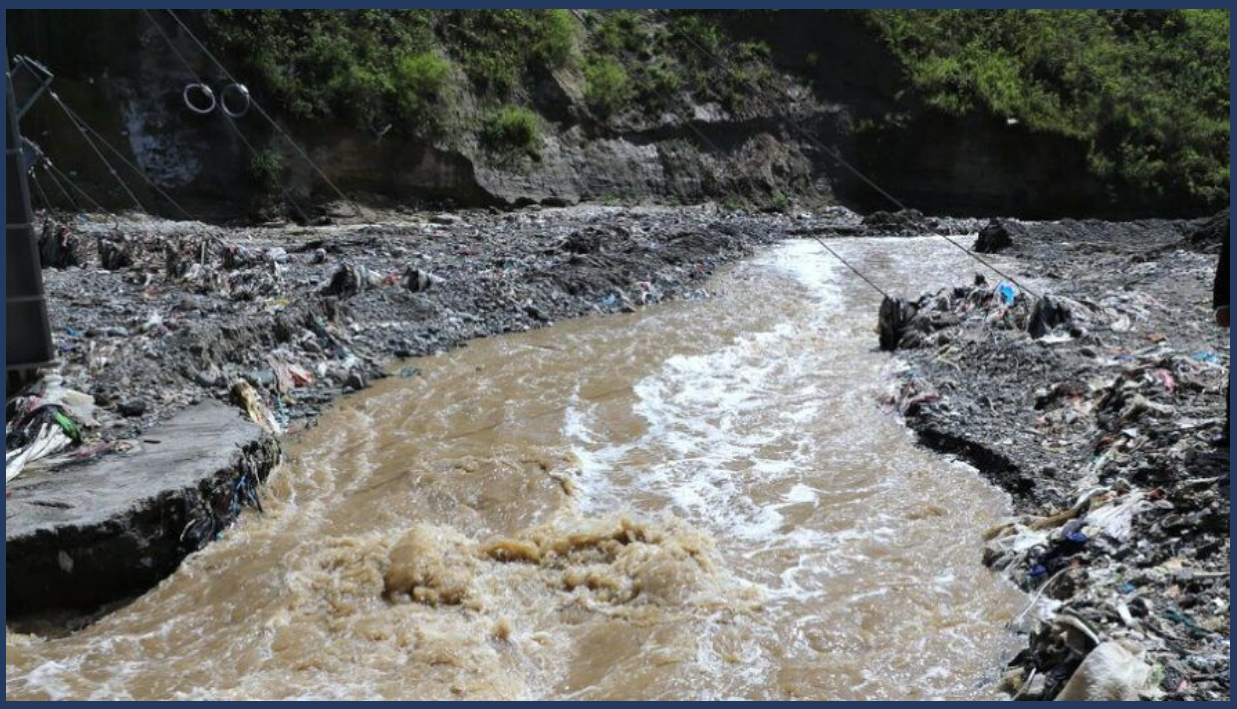

TU Delft

Witteveen + Bos

Assessing the Impact of Spatially Distributed Precipitation on Hydrological Modelling in Data-Scarce Mountainous Basin

Case Study: Rio Las Vacas

by

Muhammad Rifki Rasyid

to obtain the degree of Master of Science
at the Delft University of Technology
to be defended publicly on 23 August 2024

Thesis committee:

Chair:	Prof. Dr. Thom Bogaard
Supervisors:	Dr. Gerrit Schoups
Examiner:	Michel Zuijderwijk, MSc (Witteveen+Bos)
	Bart Dekens, MSc (Witteveen+Bos)
Place:	Faculty of Civil Engineering and Geosciences, Delft
Project Duration:	12 months
Student number:	5462924

An electronic version of this thesis is available at `http://repository.tudelft.nl/`.

Faculty of Civil Engineering & Geosciences · Delft University of Technology

Preface

This thesis describes my MSc thesis project and is written to obtain the Master of Science in Civil Engineering - Water Management degree at Delft University of Technology. I carried out this research project with the help of my supervisors from the Delft University of Technology and the Water Nuisance group of Witteveen+Bos. The thesis project aims to improve the hydrological model in a scarce basin using various precipitation products and assessing its performance. The topic was proposed by Witteveen+Bos and developed together with my supervisors at TU Delft.

During my thesis project, I had a lot of help from many people at Delft University of Technology and Witteveen+Bos. Therefore, I would like to thank several people for contributing to my project. First of all, I express my deepest gratitude to my thesis committee, Thom Bogaard, Gerrit Schoups, Michel Zuiderwijk and Bart Dekens, who have provided me with their knowledge, guidance, expertise, and time throughout the thesis period. I also want to thank Diana Agudelo and Linnaea Cahill, who helped me with their network in Guatemala and assisted me in procuring new data. I am thankful to the Water Nuisance group, Daan te Witt, Josje van Houwlingen, and Noortje Romeijn, for helping me adapt to the new office and understand the wflow model and how to use it. I also want to thank Pascal de Schmidt, study advisor at Civil Engineering and Geosciences, who helped me plan to catch up on my studies.

The journey to obtain a master's degree is not easy for me. Therefore, I am very grateful for the funding sponsored by the Indonesian government through Lembaga Pengelola Dana Pendidikan (LPDP). The funding helps me realise my dream of pursuing advanced education. I also want to thank the people at Witteveen+Bos Indonesia who supported and facilitated me during my studies. Lastly, I want to thank my family and friends in Indonesia and the Netherlands, who encouraged and supported me all the way through this journey.

Muhammad Rifki Rasyid
Delft, June 2024

Summary

Hydrological modelling is an essential aspect of water resources management and has many applications, particularly water quality monitoring and the pollutant transmission. Recent research found that hydrology also plays a crucial role in plastic transport from land to the ocean, making it vital to understand the impact of spatially distributed precipitation on the hydrological processes. This leads to the question of how a hydrological model can help waste management and prevent plastic waste in the ocean. However, developing a suitable hydrological model with limited data availability, complex topography, and human interaction is a challenge. This research uses the Rio Las Vacas catchment as a case study and focuses on testing the applicability of the wflow hydrological model and assessing the impact of heterogeneous precipitation on the model result.

The research analysed the ground data available in Rio Las Vacas to verify and validate its quality. This study uses precipitation gauges, ERA5, and CHIRPS to assess the most suitable input for modelling rainfall-runoff in the Rio Las Vacas catchment. The catchment's hydrology was analysed and a conceptual model of the catchment was proposed. Using the wflow model, the hydrological response was modelled using the three rainfall products and the effect of uncertainty and spatially distributed rainfall was assessed.

The result shows that the Rio Las Vacas catchment suffers from a shortage of hydrometeorological information which is also of spurious quality. Only three rain gauges were available, and their analysis revealed high error variance and independence between stations. Hydrological characterisation analysis revealed significant human-induced changes. A calibrated wflow model effectively simulated the catchment's hydrological response, demonstrating that global parameterisation was sufficient as a starting point for the model in this region. The soil water parameters are one of the most significant parameters in generating runoff for the model. The impact of spatially distributed precipitation is prominent in the model. This is one of the reasons for ERA5 to perform poorly in simulating the streamflow in the catchment. Based on the quantitative validation, the best modelling results came from using rain gauge data interpolated with the IDW method, followed by CHIRPS. However, the qualitative assessment shows CHIRPS is more reliable among the datasets.

In conclusion, this study shows the difficulties of modelling a data-scarce basin in the mountainous region. However, extensive data verification and validation, in combination with hydrological characterisation, helps to improve the model result. It also shows the precipitation inputs were crucial for a distributed model. The use of precipitation input with finer resolution could improve the model significantly. The study shows that the spatio-temporal distribution of the precipitation did not only affect the streamflow at the measurement point, but also the spatio-temporal runoff generated in the basin at pixel level. This could propagate to the water quality or plastic transport study. Among the datasets tested, CHIRPS emerged as the most reliable and suitable for hydrological modelling in this basin, both quantitatively and qualitatively.

Contents

List of Figures

List of Tables

1 Introduction

1.1. Background

Hydrological modelling is an essential aspect of water resource management and has many applications. Hydrological models are used for water resource planning, development, and management and added into coupled systems modelling, such as water quality, hydro-ecology, and climate [45]. Recent research found that hydrology also plays a crucial role in plastic transport from land to the ocean [60]. Based on a global model, it was found that 60% of plastic produced had been thrown away in landfills or the environment [40]. Much of these plastic wastes end up in the ocean, either via illegal dumping in the coastal settlement [29] or transported via river [50, 35]. Meijer et al. [40] estimated that 0.8 - 2.7 million metric tons of ocean plastic came from the river. This leads to the question of how a hydrological model can help waste management and prevent plastic waste in the ocean.

Based on its size, plastic has different mechanisms of transport from terrestrial ecosystems to the ocean. Macroplastic (size $>$ 5 mm) primary mechanism of transport would be through direct deposit, combined sewer overflow, and discharge from urban drainage system [15]. High precipitation and flooding influence overland plastic mobilisation to the river system, especially in a highly populated urbanised area [48, 15]. The source of plastic can also be traced from the very upstream of the catchment, for example, in mountainous regions [32]. River discharge also has a significant correlation, although not uniform within the river length, to the amount of plastic debris transported in the river [15]. Combining the facts, it is believed that the hydrological model, in combination with the waste monitoring results, can be used to monitor and predict the amount of plastic transported in the river.

Several actions and projects have been carried out to prevent and reduce the number of plastic waste in the sea. One of these projects is in the Rio Las Vacas basin, a tributary of the Rio Motagua River in Guatemala. Witteveen+Bos was tasked to inspect the backwater effect on the net installed in the Rio Las Vacas [23]. Because Guatemala has a major concern regarding solid waste in the river ecosystem [5]. A hydrological model could help with this problem by examining the relationship between water resource engineering and the correlation between hydrology and plastic waste in the riverine system. However, developing a suitable hydrological model with limited ground data availability is a challenge [61, 24]. The problem is aggravated towards the upstream of the catchment, where the topography leads to notoriously heterogeneous precipitation forces [2]. The interaction between humans and the catchment also adds another challenge in conceptualising the catchment's behaviour into a model [3]. These are the problems Witteveen+Bos faced when developing a hydrological model for Rio Las Vacas.

Previous study shows that spatial variability of precipitation is one of the dominant factors in runoff generation [52]. Hence, the estimation of spatially distributed precipitation as the input for hydrological modelling is one of the critical components. The local rain gauges are often interpolated to create a spatially distributed precipitation dataset. However, the accuracy of the dataset produced depends on the density of the rain gauge network available [52]. Furthermore, the geographic effect in the mountainous basin also could affect the accuracy [38]. These are the main issues in the Rio Las Vacas basin, which is located in the mountainous basin and has a sparse rain gauge network. In recent years, data acquisition in a data-scare region can be supplemented by the availability of satellite missions and reanalysis datasets on multiple variables [24]. Several studies have been conducted to determine the consistencies of the satellite-based and reanalysis datasets over various regions [21, 11]. However, the validity and consistency of these datasets might not be transferable to other regions. Hence, a separate assessment is required to discourse its reliability [21, 11].

This research focuses on improving the hydrological model set up by Witteveen+Bos in the Rio Las Vacas. The study aims to explore the effect of spatial and temporal heterogeneous precipitation patterns on the performance of the models to depict the hydrological processes in the catchment. A distributed model called wflow was used in this research to model the hydrological processes in the mountainous basin of Rio Las Vacas, Guatemala. This study's outcome is expected to verify the ground data available and use the capabilities of the wflow model to simulate the streamflow of the Rio Las Vacas catchment.

1.2. Research Question

Developing a reliable hydrological model to simulate discharge in data-scarce regions is challenging. Furthermore, the quality of available ground data is also vague, increasing the uncertainty of the model. Therefore, this study aims to gain insight into developing the hydrological model in the mountainous basin with the limited available data. This leads to the following research question and associated sub-questions: **"How to improve hydrological modelling in data scarce and highly heterogenous precipitation patterns basin?"**

The study will address the main research question through a series of sub-questions. The following sub-questions are formulated as follows:

SQ1: How to verify and validate the quality of the ground data?

The data scarcity is one of the challenges in building a hydrological model. Data scarcity is not limited to the quantity but also the quality of the data. The Rio Las Vacas has several available ground data in the form of rain gauges and river measurements. However, the data contains gaps, and the quality of the measured values is unknown. This first question aims to verify and validate the quality of available ground data in the Rio Las Vacas basin. This step also helps to understand the hydrological characteristics of the catchment.

SQ2: How to select the appropriate precipitation forcing data for the model?

The limitation of the ground data is the extent of the represented area, which is aggravated by the number of ground stations that cover the catchment. Mountainous regions are known for their heterogeneous precipitation. This sub-questions explore how the ground station data and other data sources, such as satellite or reanalysis data, can be used for the hydrological model.

SQ3: What is the hydrology characteristic of Rio Las Vacas basin?

Hydrological modelling requires assumptions and several parameter settings to obtain the model output. These assumptions and parameterisation are crucial parts of the hydrological model formulation. Therefore,

these assumptions and parameters should be based on the catchment's hydrological characteristics. This step will give insight into the catchment's characteristics, thus leading to the assumption used in‘ the model.

SQ4: Comparing precipitation forces dataset; which simulates the discharge the best?
The advantage of using a distributed model such as wflow is that it can conceptually simulate the processes in the catchment areas using discrete grids. Therefore, the model can test the effect of precipitation force heterogeneity on the streamflow. This sub-question compares and explores the model output using different precipitation forces and determines the most suitable dataset.

1.3. Structure of the Report

This report will be separated into several chapters. **Chapter 2** will cover the study area description and the data sources. This research methodology will be explained in **Chapter 3**, including the study sites, the used dataset, and model structures. The result of this research will be covered in **Chapter 4**, where the impact on the hydrological model and waste transport will be shown. **Chapter 5** discussed the results overall and their implications. Lastly, the report will be closed in **Chapter 6** with the research's conclusions, recommendations and limitations.

2

Study area and data

2.1. Site description

2.1.1. Guatemala

Guatemala covers 108.890 square kilometres and is divided into three main drainage basins: the Pacific Ocean, the Caribbean, and the Gulf of Mexico [55].

The country's geography ranges from a coastal plain in the south to a volcanic mountain dispersed from west to east, dominant in the country's central area [55]. The country's landscape comprises narrow coastal plains, rolling limestone plateaus, and mountains [55]. The main physiographical feature of the area is the Inter-American Andean Mountain range (Sierra Madre), which crosses from northwest to southeast [55]. This range can then be divided into four main geographical areas: two lowland areas and two mountain systems. The lowland areas are: (1) the Peten and Belize lowlands, which have a typical karst topography with altitude varies up to 600 meters; and (2) the Pacific coastal belt, from 25 to 50 km wide in the southern part with altitudes up to 500 m above sea level. The two mountain systems are: (1) a volcanic mountains range adjacent to the Pacific Coast, comprising 33 volcanoes with maximum heights of 3.000 to 4.200 m above sea level; and (2) the Cuchumantanes, Chama, and Las Minas massifs and have summits as high as 3.800 m above sea level. The Rio Motagua flood plain and the Caribbean coast's low-lying coastal plains comprise most of the topography.

Because the area is dominated by mountainous terrain, the weather is influenced and varies accordingly. Weather systems and prevailing winds generally move from west to east of the country. The area has a tropical climate with distinct wet and dry seasons. The wet season extends from early May through October, while the rest of the year is dry. The wet season usually begins slightly earlier in April [55]. The local meteorological stations show more heterogeneous precipitation between July and December [54]. The smaller stream dries up, and stream flows decline during the dry season, especially in the highlands. Most of the country's highland and more minor stream basins experience drought conditions from late February until the beginning of the wet season in May.

2.1.2. Rio Las Vacas Basin

The Rio Las Vacas basin is one of the tributaries of the Rio Motagua basin, part of the Caribbean Sea basin. The Rio Las Vacas basin flows from the mountain into the Hidrovacas Dam with a total area of 235 km^2 [17]. However, the study uses the basin derived from the DEM (see Fig. **2.1**) with a catchment area of

276 km^2. The Las Vacas basin is part of the Guatemala Metropolitan Region (GMR) and is characterised by a constant increase in urbanisation. The river supports approx. 2 million people that live within GMR [5]. The area's landscape ranges between 1.127 - 2.257 m above mean sea level and features steep slopes that carry landslide risk [30]. The highland area of the catchment is dominated by an urban area, covered for around 30%, while the rest of the area is covered by a combination of shrubland, grassland and tree cover [1]. The precipitation is between 1.2 to 1.7 m per year, with the average discharge of 4 - 8 m^3/s in the wet season and 2 - 4 m^3/s in the dry season [5]. The wastewater effluent from Guatemala City also influences the river discharge [5]. The area's geological formations are volcanic, metamorphic and sedimentary rocks. Depending on the composition and characteristics of the soil, these formations support the water infiltration into the soil [17]. The groundwater unit of the area consists of local and shallow aquifers [47]. Fig. **2.1** presents the catchment area up until Hidrovacas Dam.

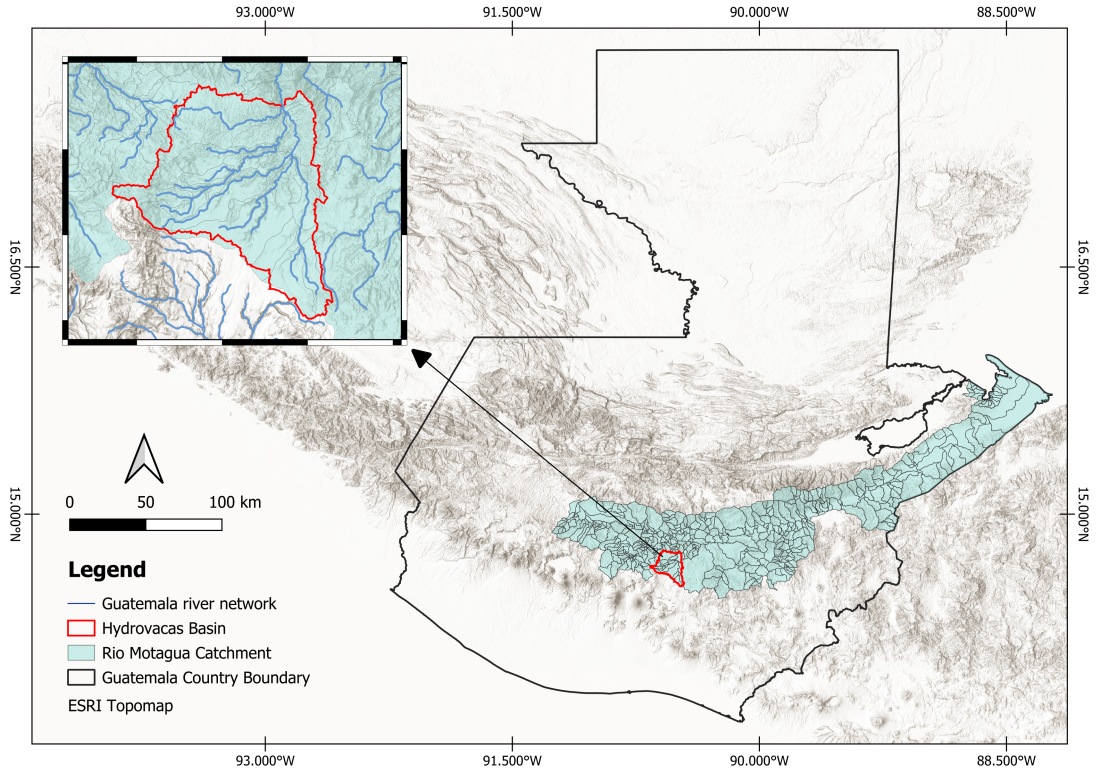

Figure 2.1: Location of the study area within Rio Motagua basin

2.2. Static input data

The static input data includes topography and land use. Both inputs are assumed to be constant because morphological changes are usually slow and do not significantly change during the modelling period. Although land use has a faster change rate over time compared to topographical change, it is also assumed to be constant. These assumptions are made to keep the hydrological model feasible.

2.2.1. Topography

The flow direction and water movement within a catchment were derived from the topographical map. MERIT Hydro is used to build the base wflow model. MERIT Hydro is a flow direction map based on MERIT DEM and the latest water layer data [63]. Besides MERIT Hydro, the study also uses the SRTM

data as a supplement. The SRTM data was used for the precipitation interpolation analysis because the data has been widely used for the interpolation analysis [53, 36]. The SRTM data has a resolution of 90 m and vertical accuracy of 16 m [42]. Fig. **2.2** is presented the DEM of the study area.

2.2.2. Land use

The land use data will determine how the catchment responds to rainfall. This study uses the GlobCover 2009 as the land use input for the hydrological model [1]. GlobCover 2009 is a global land cover dataset derived from satellite imagery acquired by the Medium Resolution Imaging Spectrometer (MERIS) sensor aboard the European Space Agency's Envisat satellite.

GlobCover 2009 offers information that is needed in the hydrological model. For example, the dataset covers a wide range of land cover classes, distinct into classes, including tree cover, croplands, urban areas, and bare soil. The comprehensive coverage enables the representation of different land use types and their respective hydrological response, allowing more realistic simulation in hydrological modelling. Fig. **2.2**

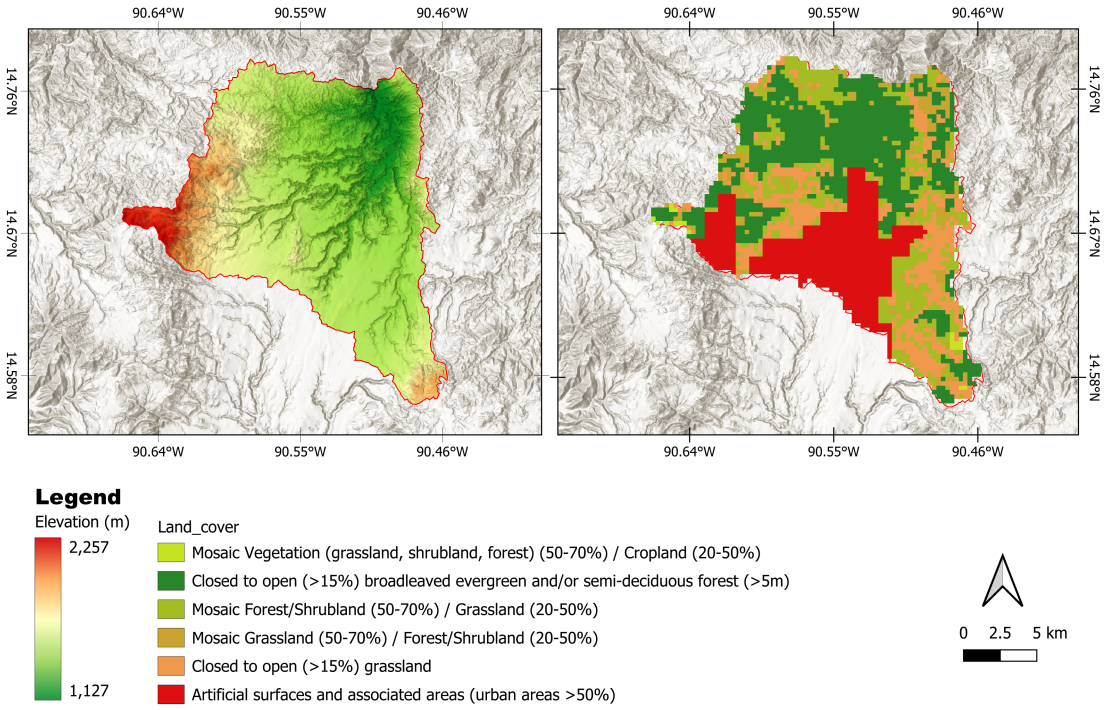

Figure 2.2: DEM (right) and Land Use/Land Cover (left) of the study area

2.3. Dynamic input data

2.3.1. Precipitation

The Rio Las Vacas basin has a sparse precipitation monitoring network, making defining precipitation challenging. The precipitation pattern is also spatially complex, with differences in precipitation amounts over short distances, especially along the mountain ranges [44].

The local measurements were obtained from four meteorological stations around the catchment area

(Fig. **2.7**. The data from the three meteorological stations (INSIVUMEH, San Pedro Ayampuc, and Suiza Contenta) were available from 2009 - 2019. The Aurora Airport station data has an hourly basis from 2000 to 2019. The local measurements allow for the study of the significance of variation in precipitation on temporal and spatial scales. However, since all the stations are located outside the catchment area, it is still a challenge to create reliable interpolation to create spatial representation over the catchment, especially in Guatemala City, which is located in the foothills where the weather patterns are influenced by the topography of the area [2].

2.3.2. Potential Evaporation

The potential evaporation data used for the model was obtained using the De Bruin formula based on the meteorology data obtained from ERA5. Using this method, the potential evaporation could be downscaled from ERA5 resolution to the model's grid size using corrected temperature lapse rate and solar radiation data. The potential evapotranspiration from ERA5 is presented in Fig. **2.5**. In addition, the potential evaporation data is also derived from temperature from one meteorological station, the Aurora Airport, which provides the hourly temperature data (see Fig. **2.4**). The method to estimate potential evaporation from temperature data is presented in Subsection **3.1.3**. The potential evaporation derived using the Hargreaves equation ranges between 0.7 - 7.8 mm/day. This range is also in line with the data obtained from ERA5. However, reflecting on the timing and magnitude of precipitation inconsistencies in the Aurora Airport stations, the potential evaporation is also compared to the ERA5 data. Fig. **2.3** compares the evaporation derived from Aurora Aiport and ERA5. It shows no correlation between both data.

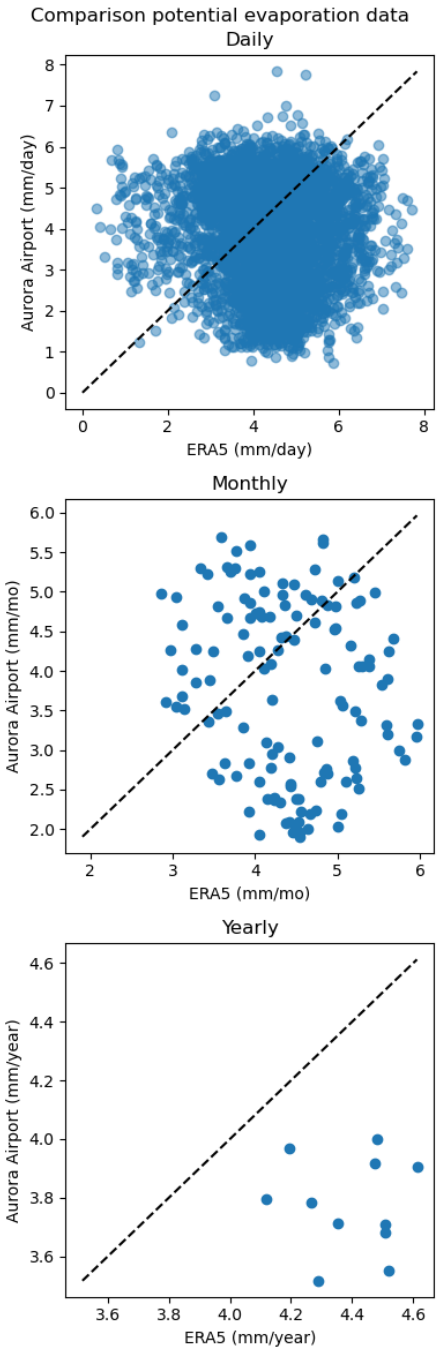

Figure 2.3: The comparison of ERA5 and Aurora Airport data.

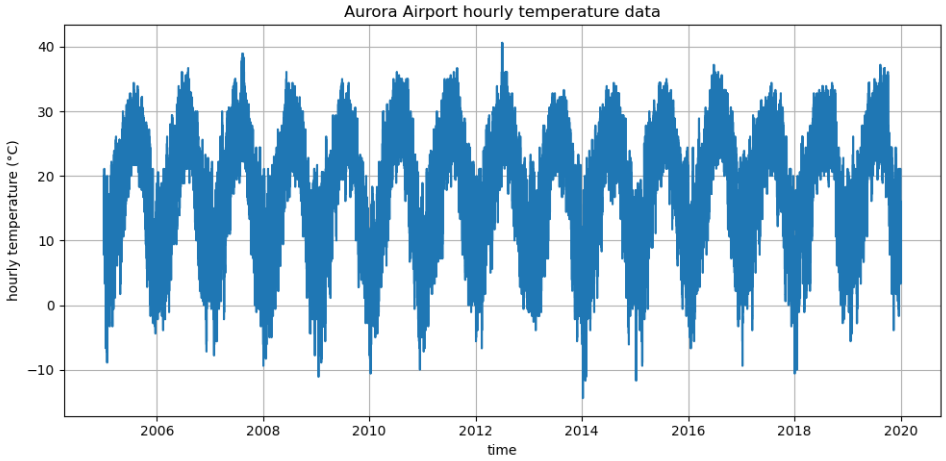

Figure 2.4: Hourly temperature data of Aurora Airport from 2005 - 2019

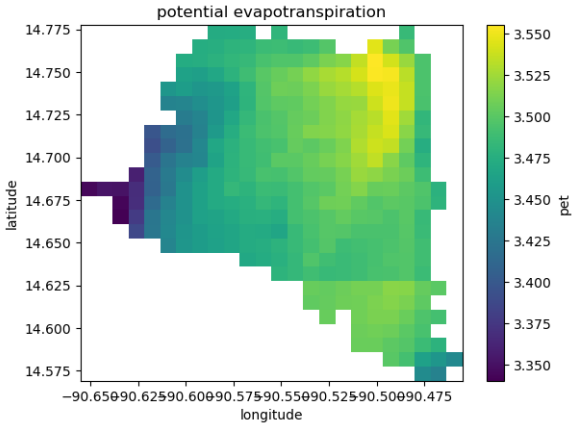

Figure 2.5: Mean potential evapotranspiration using the meteorology data from ERA5

2.3.3. Streamflow

The streamflow data is a daily average discharge measured in m^3/s from 2005 to 2019. This data was obtained indirectly from Universidad del Valle's research for the same catchment [28]. Based on correspondence with local experts, the noise could be the result of the mini hydropower generator upstream of the measurement point. However, the location of this mini hydropower generator was not specified and could not be pinpointed on the map due to its size. The streamflow is also influenced by the wastewater effluent of the Guatemala Metropolitan Region [5, 17]. The data from Universidad del Valle is also compared to the primary data obtained from the dam operator through Witteveen+Bos. However, since the primary data length is limited to 2021 to 2022, the validation check only deals with the magnitude of streamflow. Fig. **2.8** presents the comparison between the data from the university has the same magnitude as the data obtained from the dam operator. The complete streamflow data and its measurement location are presented in Fig. **2.6** and Fig. **2.7**.

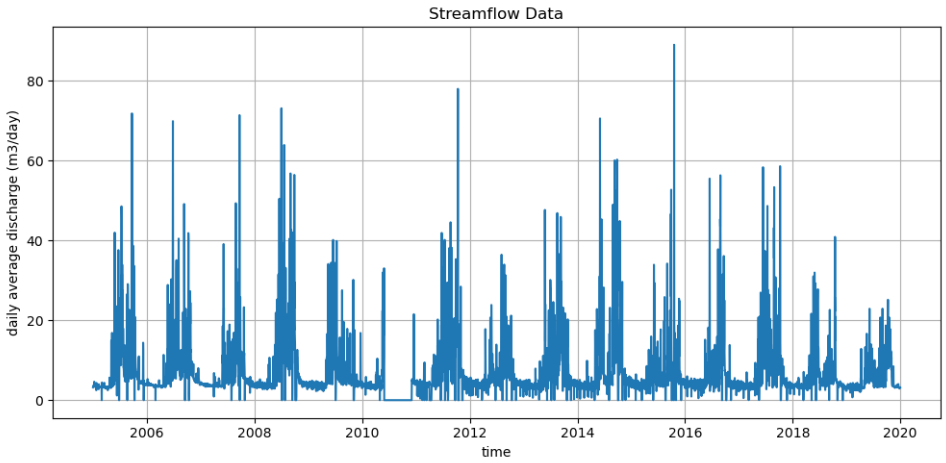

Figure 2.6: Full time-series of streamflow data at Hydropower Dam - Rio Las Vacas

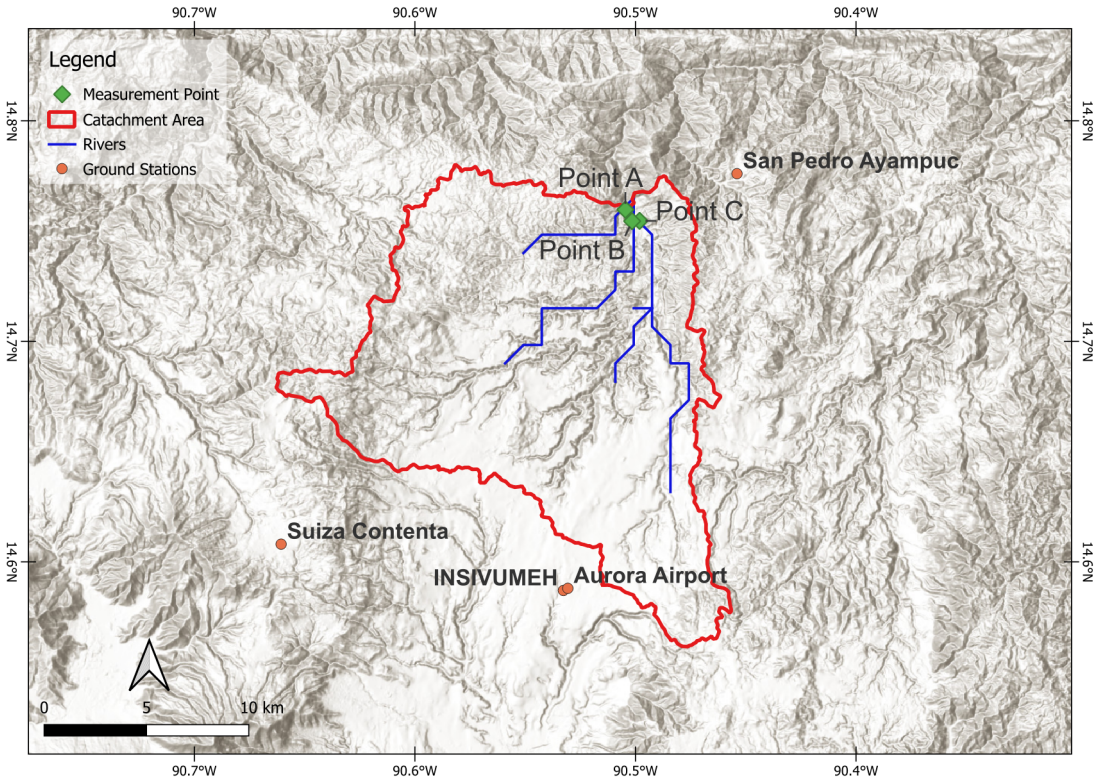

Figure 2.7: The streamflow measurement and ground stations location

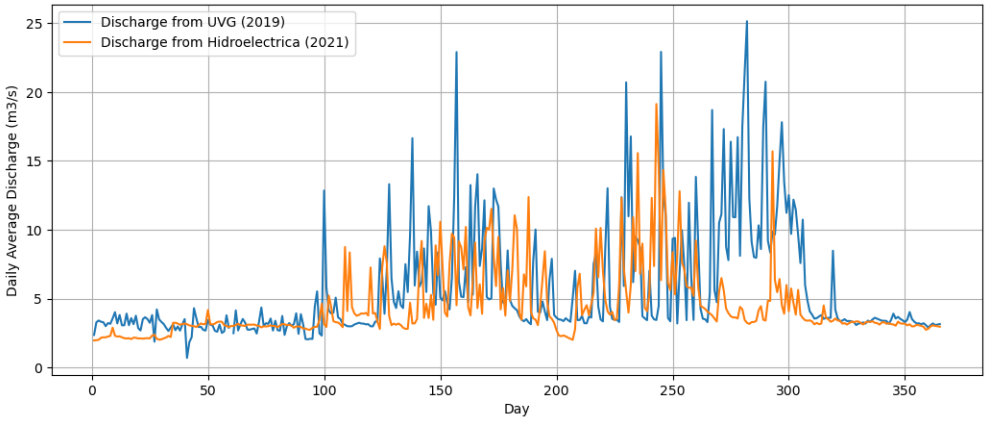

Figure 2.8: The comparison between discharge obtained from Universidad del Valle in 2019 and Hidrovacas Dam operator in 2021

3

Methodology

This chapter describes the methodologies and approaches used in the study. Fig. **3.1** presents the Overview of all steps to achieve the final results.

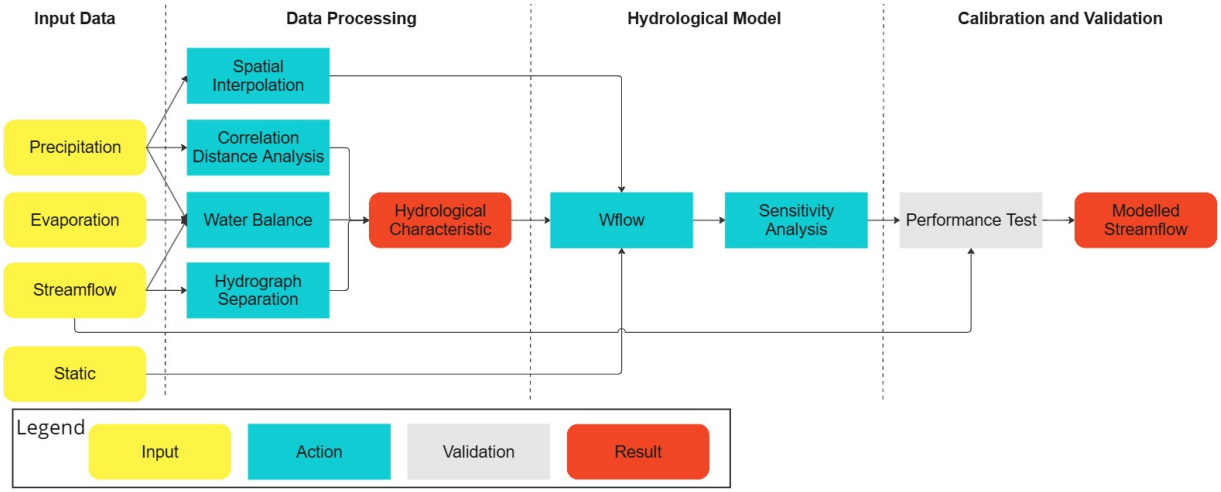

Figure 3.1: Overview of the modelling study

3.1. Hydrological charaterisation

This section describes the analysis method characterising the Rio Las Vacas Basin. Several analyses of the catchment were carried out to check the fitness of the dataset to be used for the model. The data assessment will focus on the ground stations and the remote-sensing data as a supplement.

3.1.1. Double Mass Analysis

The main objective of double mass analysis is to check the consistency of the data from the rain gauge [9]. The study plotted the cumulative rainfall from each station against the mean of all rain gauge networks. The inconsistencies in the data show when the gradient of the plot changes in time. When the gradient did not change, the data of the rain gauges was considered consistent.

3.1.2. Correlation-distance analysis

However, the rain gauge is only representative of a limited spatial extent [56]. Therefore, a correlation analysis within the rain gauge network was performed to determine the spatial variability of the precipitation in distance. The correlation in distance often can be expressed by negative exponential function as follows [7]:

$$\rho_i = \rho_0 \exp\left\{-\frac{r}{r_0}\right\} \tag{3.1}$$

Where ρ_i represents correlation at a distance r, ρ_0 represents correlation at a distance 0, r represents the distance between stations, and r_0 is a length scale defining the rate at which the correlation decreases.

From the above equation, the relative error in the areal rainfall estimation can be quantified using the following equation [12]:

$$Z_{areal} = C_v \sqrt{\frac{1}{N}\left(1 - \rho_0 + \frac{0.23}{r_0}\sqrt{\frac{S}{N}}\right)} \tag{3.2}$$

Where Z_{areal} represents relative variance error in areal rainfall estimate, C_v for the coefficient of variation, S for catchment area in km^2, and N for a number of gauging stations.

This relative variance error can be seen as a function of variation in time series, spatial correlation, and match between the basin size and number of observation gauges. Reflecting on the formula, higher temporal variation (in the form of C_v) will result in higher variance error, requiring a denser network or higher permissible error.

3.1.3. Evaporation estimation

Due to limited local measurement data, estimating the evaporation around the study area has been challenging. This study uses the Hargreaves equation to estimate potential evaporation. The Hargreaves equation has a simpler data requirement, extraterrestrial radiation and temperature, to estimate the potential evaporation [19]. This formula is an acceptable method from the guideline by FAO for limited data availability[16]. The estimation using the Hargreaves formula will be used to study the water balances based on the ground station data. The extraterrestrial radiation in the measurement station can be estimated using the following equation:

$$R_A = \frac{24(60)}{\pi} G_{sc} d_r [\omega_s sin(\phi) sin(\delta) + cos(\phi) cos(\delta) sin(\omega_s)] \tag{3.3}$$

Where R_A represent the extraterrestrial radiation, G_{sc} for solar constant, d_r for inverse relative distance Earth-Sun, ω_s for sunset hour angle, ϕ for latitude in rad and δ for solar decimation. Then, the potential evaporation was estimated using the extraterrestrial radiation and temperature data from the local measurement station using the following equation:

$$ETP = 0.0023 * R_A * T_D^{0.5}(T_C + 17.8) \tag{3.4}$$

Where ETP represent the Evapotranspiration Potential, T_D is the difference between the daily maximum and minimum temperature, and T_C is the daily mean temperature.

The potential evapotranspiration grid cells for the model are estimated using the global radiation and temperature data from ERA5. The temperature data is then scaled based on elevation. The estimation

used the De Bruin formula [10] as presented in Fig. **2.5**.

3.1.4. Water Balance

The water balance analysis was used to understand water partitioning within the catchment. The water balance was used to understand the hydrologic system of the catchment [64]. The water balance model in this analysis was conducted using the simple bucket model where the catchment was assumed as a bucket which will be filled by precipitation and emptied by evaporation and discharge [64]. The model is expressed as follows:

$$\Delta S = P - E - Q \tag{3.5}$$

where S represent storage in catchment, P for precipitation, E for actual evaporation, and Q for discharge. Because the analysis was conducted using long-term water balance, the change in storage ΔS became negligible. Therefore, the model becomes a function as follows:

$$0 = P - E - Q \tag{3.6}$$

The data available did not have the actual evaporation. Hence, a coefficient was applied to the potential evaporation to obtain the actual evaporation. The model is expressed as follows:

$$0 = P - frac * PET - Q \tag{3.7}$$

The $frac$ value was obtained iteratively using long-term precipitation and discharge to reach equilibrium.

The long-term water balance was also calculated using the Budyko framework. The Budyko framework is based on the idea that the long-term average actual evaporation was mainly determined by the balance between the precipitation and potential evaporation [57]. The Budyko framework uses the equation as follows to estimate the average actual evaporation [6]:

$$\frac{E_A}{P} = \left[\frac{E_P}{P} tanh\left(\frac{E_P^-1}{P}\right)\left(1 - exp\left(-\frac{E_P}{P}\right)\right)\right]^{0.5} \tag{3.8}$$

Where E_A, E_P, and P are the long-term actual evaporation, potential evaporation, and precipitation, respectively. Budyko, 1974 argues that all catchments should be located near his proposed curve [6]

The data used for the water balance analysis will be solely based on ERA5 data. Despite the complete data requirement to conduct a water balance analysis, the Aurora Airport data has too much uncertainty and inconsistencies to be used. The data used for the study is from 2011 to 2019. The reason for not using the entire time series for the water balance is because of a significant measurement error in the streamflow data during the 2010 time frame. Therefore, maintaining consistency and continuity was considered enough to keep the water balance from 2011 to 2019.

3.1.5. Hydrograph Separation

A hydrograph separation was conducted to gain more insight into the catchment area. The hydrograph separation could be used to see how the catchment responds to the precipitation [4]. Furthermore, the result of hydrograph separation could also be used to tackle the equifinality that might happen during the model evaluation and calibration process [8, 59]. The method used for this separation uses WETSPRO developed by KU Leuven, based on Willems, 2009 [59].

3.2. Spatially Distributed Precipitation

The limitation of the ground station is that the ground station only represents a set of areas around the station. Therefore, when used for a distributed model, the ground station data needs to be interpolated to obtain spatial coverage of the catchment area. Several interpolation methods are commonly used: Thiessen polygons, Kriging, Linear Regressions and Inverse Distance Weighing (IDW). Due to spatially heterogeneous precipitation patterns and limited data, interpolation has been challenging. Kriging and its variance could not be used due to the limited number of ground stations available for the method. This study uses IDW and multiple linear regression (MLR) as interpolation methods because the advantages vary on a spatial scale. Compared to the Thiessen polygons, which assign the same value to the whole polygons, this method can overlook the local precipitation compared to IDW and MLR. The IDW method is expressed in the equation as follows:

$$z = \frac{\sum \frac{z_i}{d(x,x_i)^p}}{\sum \frac{1}{d(x,x_i)^p}} \tag{3.9}$$

The MLR approach employs satellite or reanalyses product, DEM properties (elevation, latitude, longitude), and ground station data to estimate precipitation in the catchment area [53, 46]. This approach has an advantage over the IDW approach for the limited amount of ground stations due to the inability to carry out cross-validation for IDW results. In the MLR approach, the satellite/reanalyses product was downscaled based on the model formula presented in Eq. (3.10), then validated on each ground station using the performance criteria given in Subsection **3.3.2**.

$$P_i = a_0 * P_{rs} + a_1 * Elevation + a_2 * Latitude + a_3 * Longitude + a_4 \tag{3.10}$$

Where P_i for the estimated precipitation at location i, P_{rs} for the precipitation from satellite/reanalyses product at location i, Elevation for the elevation (in m) at location i, latitude and longitude for the coordinate at location i in decimal degree, and a's for the parameters that will be estimated using Markov-Chain Monte Carlo simulation.

In addition to the interpolation of local rain gauges, two global datasets were also used in this study. The first one is ECMWF Reanalysis 5th generation (ERA5), a reanalysis product produced by the Copernicus Climate Change Service (C3S) at ECMWF [22]. ERA5 combines historical observations into global estimates using advanced modelling and data assimilation systems. The ERA5 model and algorithm produce meteorological data of the earth, including precipitation and potential evaporation. ERA5 have a grid size of 0.25° x 0.25° (approx. 31 x 31 km) and contains hourly values ranging from 2009 to 2021. The ERA5 dataset represents the reanalyses data [21].

The second one is The Climate Hazards Group Infrared Precipitation with Stations (CHIRPS) dataset, a satellite product developed by the Climate Hazards Center (CHC). The CHIRPS dataset combines satellite, local observation, and climate model data. The method employed caused CHIRPS to have more events and less precipitation per event [18]. The spatial and temporal variability of the data has been studied and shows aligned results on similar topography and climate [37]. The data produced has a grid size of 0.05° x 0.05° (approx. (5.5 x 5.5) km) and daily values ranging from 2009 to 2021. The CHIRPS dataset represents a combination of gauge, satellite and reanalysis data [21].

3.3. Hydrological model

The study used a distributed hydrological model package called Wflow. Wflow is a distributed hydrological model package developed by Deltares [49]. The model is programmed in the Julia language, with the software available online under the MIT License (open source). The Wflow has several model packages inside, with a certain set of parameters to be calibrated. Wflow is used because of its capability to carry out a distributed hydrology model. The distributed model discrete the model's space into the grid-cell size and performs calculations independently before compiling it according to its routing mechanism [26, 49]. A distributed model can help catch the forcing heterogeneity in the area [26].

This study uses the wflow_sbm package. The model discrete the catchment into grid cells with eight flow directions (D8) to manage surface and subsurface flow routing. The model operates under two primary concepts to simulate the discharge. The first is the vertical concept, which includes precipitation-snow, rainfall interception, and soil water process routines. The vertical routines process the water entering the model in each grid cell. The second concept is the lateral concept, which involves flow generation. The lateral concept uses the kinematic wave function to route the subsurface, overland, and river flows according to the D8 directions [49, 58]. The schematic of wflow_sbm processes is presented in Fig. **3.2**

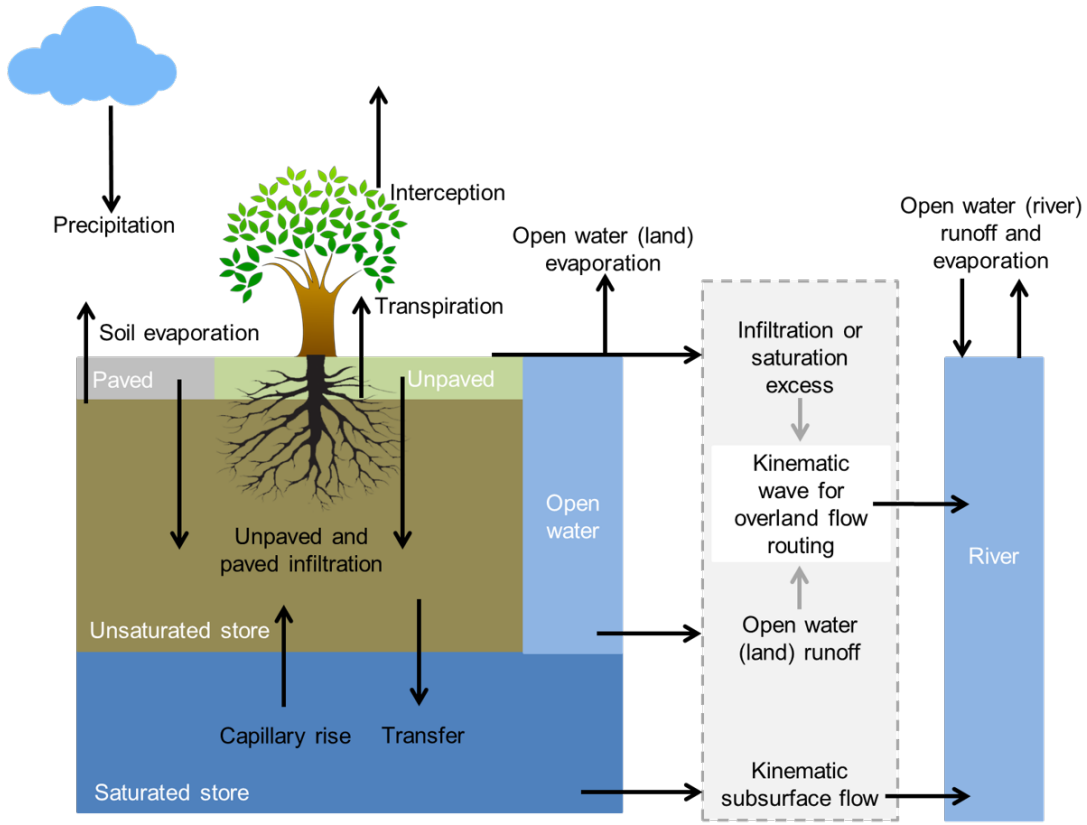

Figure 3.2: The schematisation of land-river connection within wflow_sbm model [49]

3.3.1. Calibration

The initial value of the base model parameters was set up using the global parameterisation available for wflow [58, 49, 27]. The model calibration was then conducted to fine-tune the model performance. The wflow has a large set of parameters, and because of that, several parameters were selected to be used in the calibration. These parameters were selected based on the expert's knowledge at Witteveen+Bos,

wflow documentation and literature [62, 49, 27]. Table **3.1** presents the selected parameters, what they represent, and their influence. The calibration was conducted by scaling the combination of parameters from a wide range and then narrowing it down based on the performance criteria to obtain the best set of parameters for the model. The ERA5 dataset of 2012 was used for the calibration due to the limited length of data available for the study. This period was selected because it was the largest event from the available data.

Table 3.1: Wflow calibration parameters

Parameters	Description	Effect
KsatHorFrac	Horizontal hydraulic conductivity at the surface of the soil	Height of peak flows and base flows
KsatVer	Vertical hydraulic conductivity at the surface of the soil	Height of peak flows and base flows
f	Scale decay parameter of Ksat over soil depth	Regression of peak flows
N	Manning roughness of land cells	Timing of peak flows
N_river	Manning roughness of river cells	Timing of peak flows
MaxLeakage	Maximum leakage of water that goes outside the model	Height of peak and water loss

3.3.2. Validation

The model result will be assessed against the observed discharge to determine its performance and efficiency. The metrics used for this were Nash-Sutcliffe Efficiency (NSE), Kling-Gupta Efficiency (KGE), and cumulative discharge [43, 20].

The Nash-Sutcliffe Efficiency has been widely used in hydrology studies as a validation metric. Eq. (3.11) presents the Nash-Sutcliffe formula.

$$NSE = 1 - \frac{\sum(Q_{obs} - Q_{mod})^2}{\sum(Q_{obs} - \overline{Q_{obs}})^2} \tag{3.11}$$

Where Q_{obs} and Q_{mod} represent observed and modelled discharge, respectively.

A logarithmic variant of Nash-Sutcliffe Efficiency (NSE_{log}) was also used. The NSE is sensitive to high flow rates, especially extreme values [34, 41]. Krause et al., 2005 [34] propose using the logarithmic variant to overcome the extreme values and increase the sensitivity to the lower flow rates. The NSE_{log} formula presented as follows:

$$NS_{log} = 1 - \frac{\sum(log(Q_{obs}) - log(Q_{mod}))^2}{\sum(log(Q_{obs}) - log(\overline{Q_{obs}}))^2} \tag{3.12}$$

The model results yield reasonably excellent results for peak flows, and during low flow, situations can be discovered by combining the application of two criteria [34].

Alongside the Nath-Suttclife efficiency, the study also uses the Kling-Gupta Efficiency (KGE) to assess the overall result. The KGE addresses the limitation imposed by NSE (and NSElog) by considering not only the closeness of the match but also the similarity in variability and timing. By incorporating these additional dimensions, KGE provides a more nuanced understanding of how well the model captures the dynamics and patterns of the observed data [20]. The formula for KGE presented in Eq. (3.13)

$$KGE = 1 - \sqrt{(r-1)^2 + (\alpha - 1)^2 + (\beta - 1)^2} \tag{3.13}$$

With r for Pearson correlation coefficient, α for variability of prediction errors, and β for bias term.

These metrics have a range result of $-\infty < NSE/KGE/NSE_{log} < 1.0$. The value of 1 means the model perfectly simulates the observed discharge, while the value of zero and below only predicts the mean value. The model performs acceptably if the NSE > 0.50 and the KGE > 0.3 [33]. Both performance scores are judged as equivalent because while the KGE is more responsive to the flow pattern, the NSE and NSE_{log} are more responsive to the peak's magnitude and timing of the simulation [33]. In addition, some visual judgement is also used to help assess the model performance.

Lastly, the annual cumulative discharge of the observation and simulation is also compared. This is done to avoid relying solely on the performance-scoring test. The annual cumulative discharge is not sensitive to temporal variances, which can mitigate the disadvantages of performance scoring. It serves as an extra parameter on the model performance assessment.

3.3.3. Sensitivity analysis

The sensitivity analysis for this thesis was carried out on several parameters presented for calibration (see Subsection **3.3.1**). These analyses' results were then assessed using the performance criterion discussed in Subsection **3.3.2**. The sensitivity analyses were conducted by changing the scale of the tested parameter, while the other not-tested parameters were set to default. This analysis aims to gain insight into the significance of each parameter to the model result. The selection of parameters for this analysis was based on the expert knowledge and documentation from Witteveen+Bos and Deltares.

4

Result

4.1. Hydrological characterisation

This section describes the results of the analysis to characterise the Rio Las Vacas Basin hydrology.

4.1.1. Double mass analysis

The local measurements were then studied for their consistencies using the double mass analysis [9]. The study plotted the cumulative rainfall from each station against the mean of all rain gauge networks. The inconsistencies in the data show when the gradient of the plot changes in time. When the gradient did not change, the data of the rain gauges was considered consistent. Fig. **4.1** presents the result of the double mass plot.

In Fig. **4.1a**, the station was consistent up until the middle, where the gradient changed. This occurrence also happened on the Fig. **4.1b**, where the gradient changed and then recovered. The occurrence could result from the stations being moved or having problems [9]. However, since both stations recovered and recorded consistent data after the change, the data from both stations was considered suitable. For Suiza Contenta stations, it is considered consistent.

The data from Aurora Airport was analysed against the INSIVUMEH stations as well. Because of their adjacent location, the hypothesis was the double mass analysis should be near 1:1 to each other. The analysis result is presented in Fig. **4.2**.

The result is shown in some step-like figures. Because the INSIVUMEH station test against the average of other stations was considered consistent, some problems might have occurred at Aurora Airport station. Hence, the Aurora Airport station data was deemed inconsistent and thus could not be used for the study.

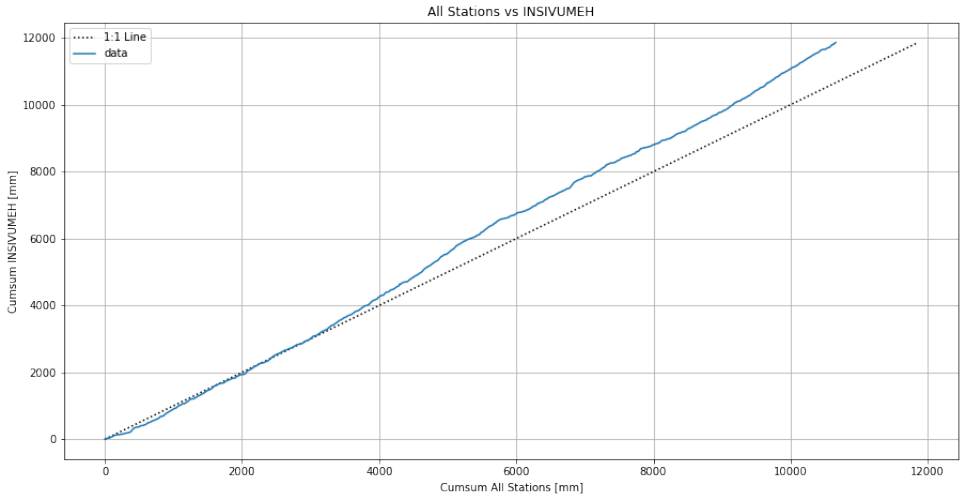

(a) INSIVUMEH station

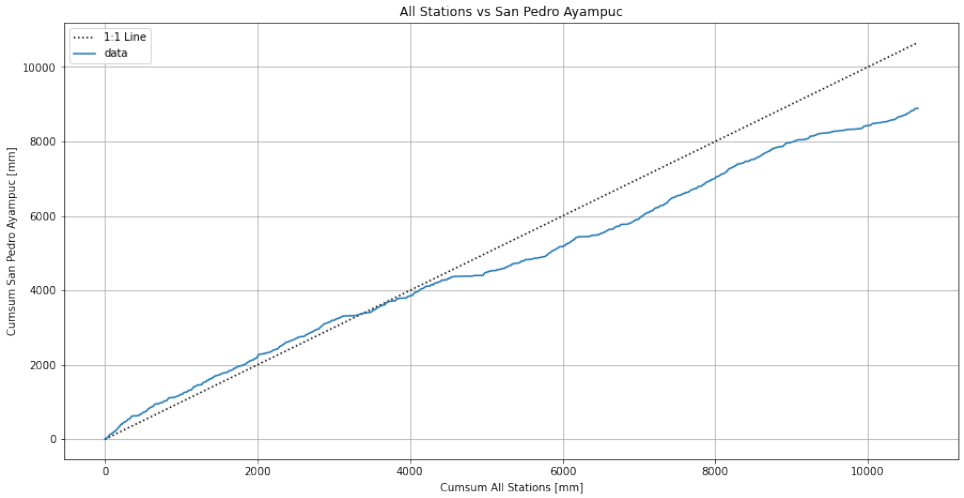

(b) San Pedro Ayampuc station

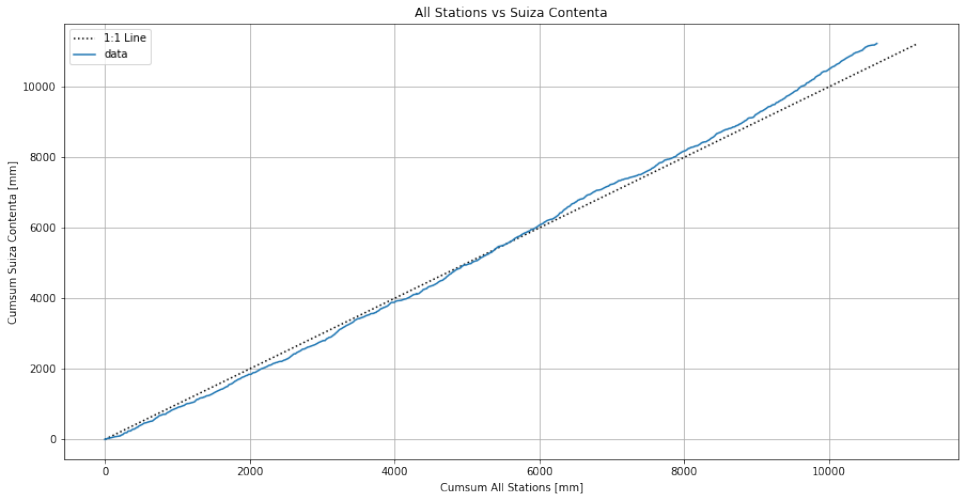

(c) Suiza Contenta station

Figure 4.1: Result of Double Mass Analysis for ground stations

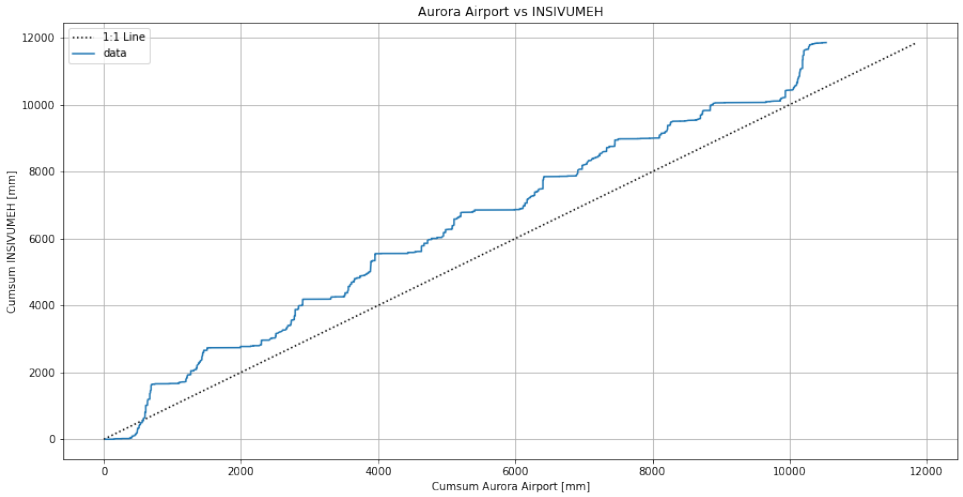

Figure 4.2: Result of Double Mass Analysis for Aurora Airport and INSIVUMEH stations

4.1.2. Correlation-distance analysis

The correlation distance of each station was assessed using daily and monthly temporal scales. The stations used are INSIVUMEH, San Pedro Ayampuc, and Suiza Contenta. This selection is based on the result of double mass analysis, which shows that these stations have the most consistent data and acceptable quality. The correlation of these stations shows a drop significantly after 20 kilometres (see Fig. **4.3**). The coefficient of variance (C_v) for both temporal scales are 2.6 and 1.1 for daily and monthly time series, respectively. The C_v is generally lower on the longer temporal due to the diminished temporal variance. However, based on the result, the C_v presented from the data shows a relatively high variance. Further investigation of the variance by calculating the relative error variance (Z_{areal}) resulted in 45% and 7% for the daily and monthly temporal scale, respectively. The error variance for the monthly temporal scale is commonly accepted due to the value below 10% [12]. The Z_{areal} for the daily basis could be reduced by adding new ground stations in the catchment. This study estimated an additional 16 ground stations were required to reduce the Z_{areal} under 10%.

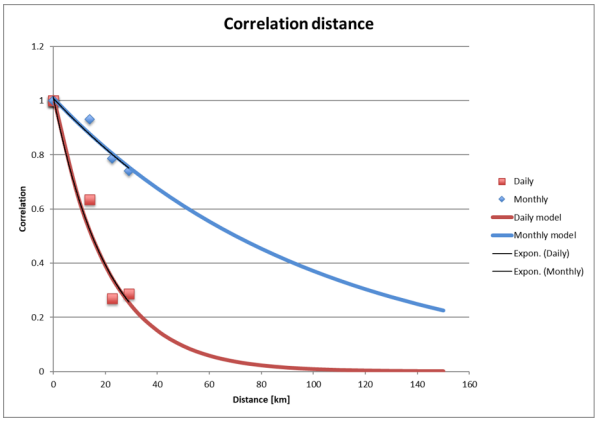

Figure 4.3: The correlation distance between three local stations shows the correlation falls significantly after 20 km

4.1.3. Hydrograph separation

Several errors and noise were found in the streamflow data inspection. The most notable error is the sudden drop in the streamflow data to near-zero value for one or several days and then returns to normal. Therefore, the first assumption made during the analysis was removing the data below 1 m^3/s. This assumption was made because the average discharge in the dry period is between 2.5 - 4.5 m^3/s [5]. The common practice for conducting the hydrograph separation is estimating the recession constant using the Master Recession Curve [25, 14, 39]. However, the data noises made it challenging to determine the MRC. Hence, the second assumption used visual inspection and trial-and-error to calibrate the low-pass filter. Although the visual inspection involves the subjectivity of the inspector and uncertainty in estimation [59].

Fig. **4.4** presents the result of the hydrograph separation with the corresponding precipitation. In the dry season of 2014 and 2017, the filter successfully fitted across the recession curve. However, in the other years, the recession slope did not match the filtered baseflow. The recession slope year-by-year was also not typical and hard to fit. For example, the recession slope gradient of the dry season of 2012 is steeper compared to the following dry season. Another example is the dry season 2016, which has the mildest slope compared to other dry seasons. The mean baseflow obtained from the separation is 3.5 $m3/s$, with a minimum of 2.6 m^3/s and a maximum of 4.5 m^3/s.

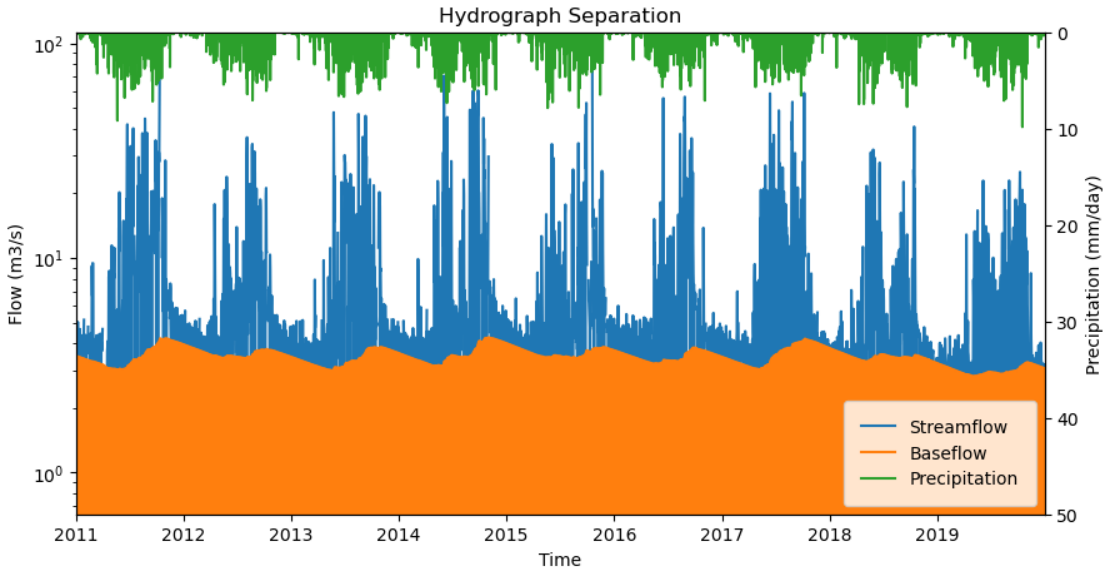

Figure 4.4: Hydrograph separation result

4.1.4. Water Balance

For the water balance analysis, the ERA5 was used. The decision to use only ERA5 data and not include the ground data was made due to the scarcity of data. The three rain gauges with consistent rainfall did not provide meteorological data to estimate the potential evaporation. Meanwhile, though the Aurora Airport has the data, the quality of the data recorded is not sufficient, as presented in **Chapter 2**. The data used for the analysis is from 2011 to 2019. The reason for not using the full-time series for the water balance is because of a significant measurement error in the streamflow data during the 2010 time frame. Therefore, maintaining consistency and continuity was considered enough to keep the water balance from 2011 to 2019. The water balance results are presented in Table **4.1**.

The result showed that the water balance did not close due to uncertainty in the data. The result showed that the E_{act}/E_{pot} value was 0.38, considered very low actual evaporation for a tropical region. The water balance based on precipitation and discharge measurement (P-Q) was then compared to the theoretical analysis using the Budyko framework to validate the result. Fig. **4.5** showed that at the y-axis, the P-Q water balance significantly differed from the theoretical approach. Both data were located at the same x-axis point due to the same potential evaporation and precipitation data used in the analysis. Further analysis was conducted by correcting the measurement data using the hydrograph separation result to remove the wastewater effluent in the discharge. P-Q water balance using the corrected streamflow resulted in a similar magnitude of evaporative index to the Budyko framework.

Table 4.1: Result of water balance using ERA5 dataset in mm/year

Year	Precipitation	Streamflow	Pot. Evaporation	Act. Evaporation	Balance
2011	1.700	915	1.531	585	200
2012	1.281	698	1.638	626	-43
2013	1.433	808	1.566	597	26
2014	1.513	920	1.589	608	-15
2015	1.293	753	1.646	629	-89
2016	1.203	732	1.641	628	-157
2017	1.447	900	1.557	595	-48
2018	1.362	647	1.645	629	86
2019	1.325	641	1.683	644	40

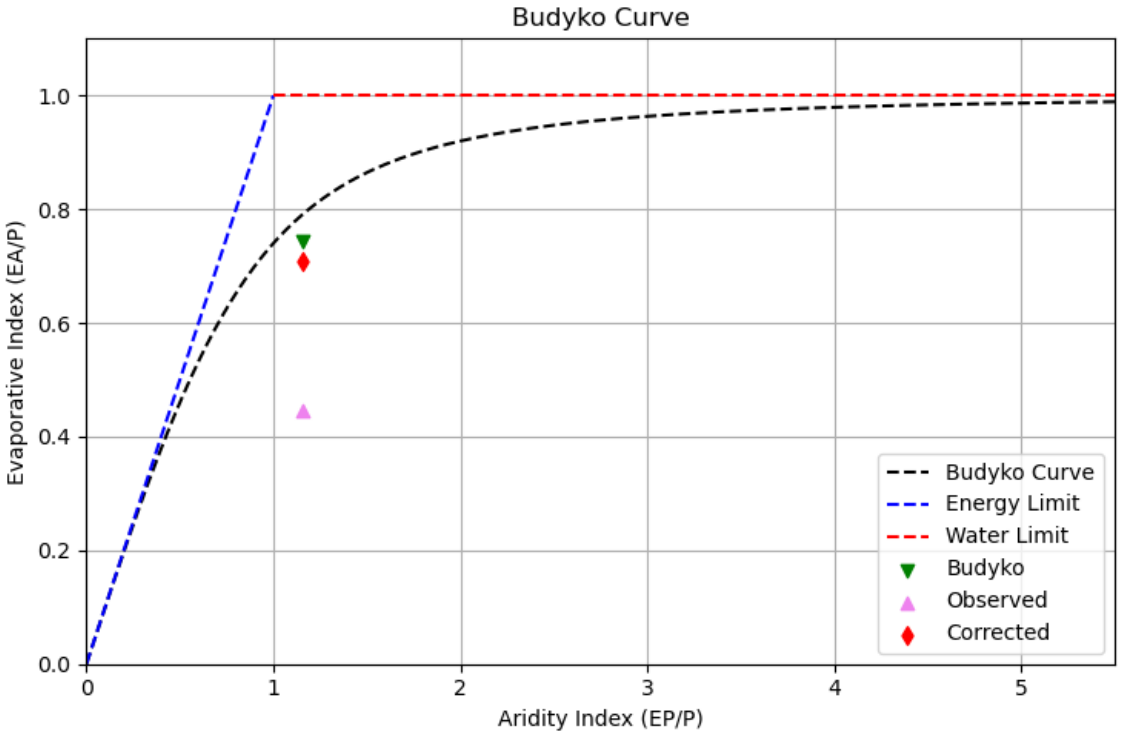

Figure 4.5: A comparison between long-term water balance calculated using Budyko framework (green), the observed P-Q (pink), and corrected Q data (red) in the Budyko curve graph

4.2. Spatially Distributed Precipitation

The local rain gauge data was interpolated using IDW and MLR interpolation methods to create a spatially distributed dataset for the area. The IDW function uses a power parameter that controls the known measurement locations that affect the interpolated values based on their distance from the observation point. In the typical case, the IDW result is cross-validated by eliminating several ground stations from the function and comparing the result to the eliminated ground station data. However, the result is used due to this study's limitation of ground stations. The MLR interpolation, on the other hand, estimates the interpolated values using the coverage data, in this case, ERA5, and DEM properties (latitude, longitude, and elevation). The parameter for MLR was obtained using the MCMC algorithm and then validated by comparing the estimated values and the ground station data. Fig. **4.6** presents the validation of the MLR interpolation. The validation result showed that the interpolation result for the monthly timescale is good enough. However, the daily timescale presented in Fig. **4.6b** shows an abysmal result.

Further, the spatial and temporal representation of each dataset was analysed. The first assessment was the temporal correlation between each dataset. Fig. **4.7** presents the scatter plot between IDW as the base and three other datasets. The scatter plot between IDW and CHIRPS shows a low correlation despite having comparable annual precipitation. This suggest that IDW and CHIRPS have differences in the timing of rainfall in the catchment. In comparison, the scatter plot between IDW and ERA5, which also shows a low correlation but exhibits tighter clusters, indicates a better temporal correlation. Another note from the temporal correlation is that the ERA5 often underestimated the precipitation compared to IDW and CHIRPS. The second assessment examined the spatial distribution of the rainfall. Fig. **4.8** presents the mean precipitation of each dataset. The ERA5's grid size is relatively large for the catchment size, which might overlook the spatial variability of the catchment. The IDW and CHIRPS, which have smaller grid sizes than ERA5, show more spatial distribution. CHIRPS and IDW show a similar precipitation distribution, where the higher altitude has more precipitation than the lower altitude. However, CHIRPS, which utilises multi-source data, shows more even and less spatial variance in the middle section of the catchment compared to IDW.

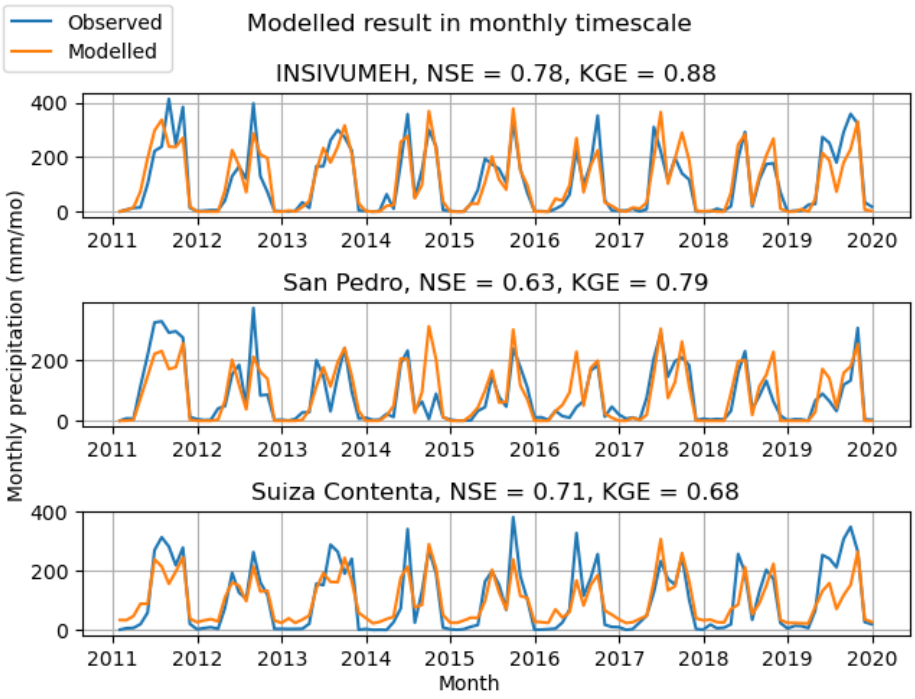

(a) Monthly interpolation

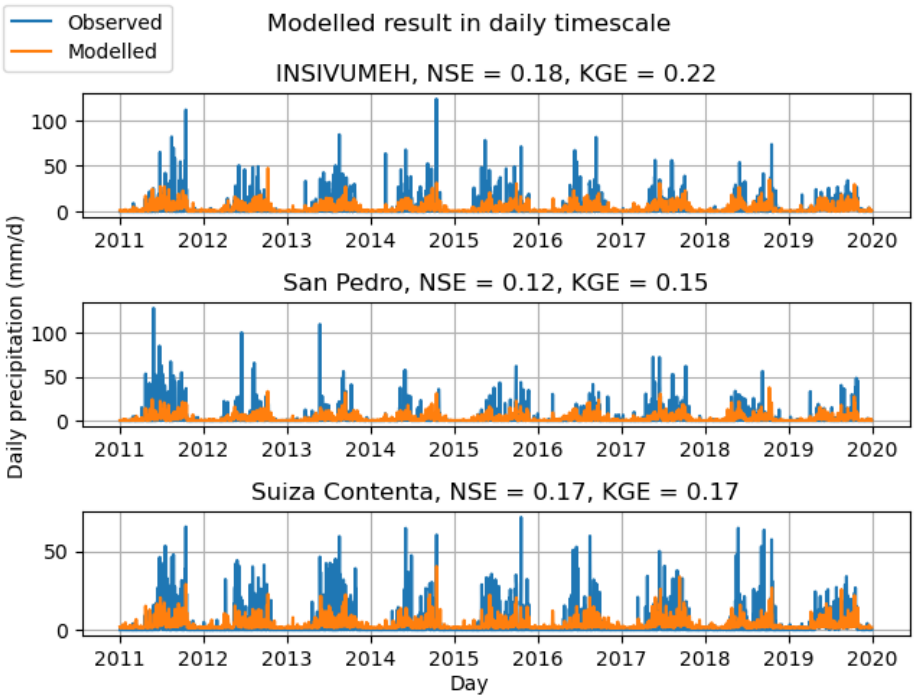

(b) Daily interpolation

Figure 4.6: MLR Interpolation result for monthly and daily timescale

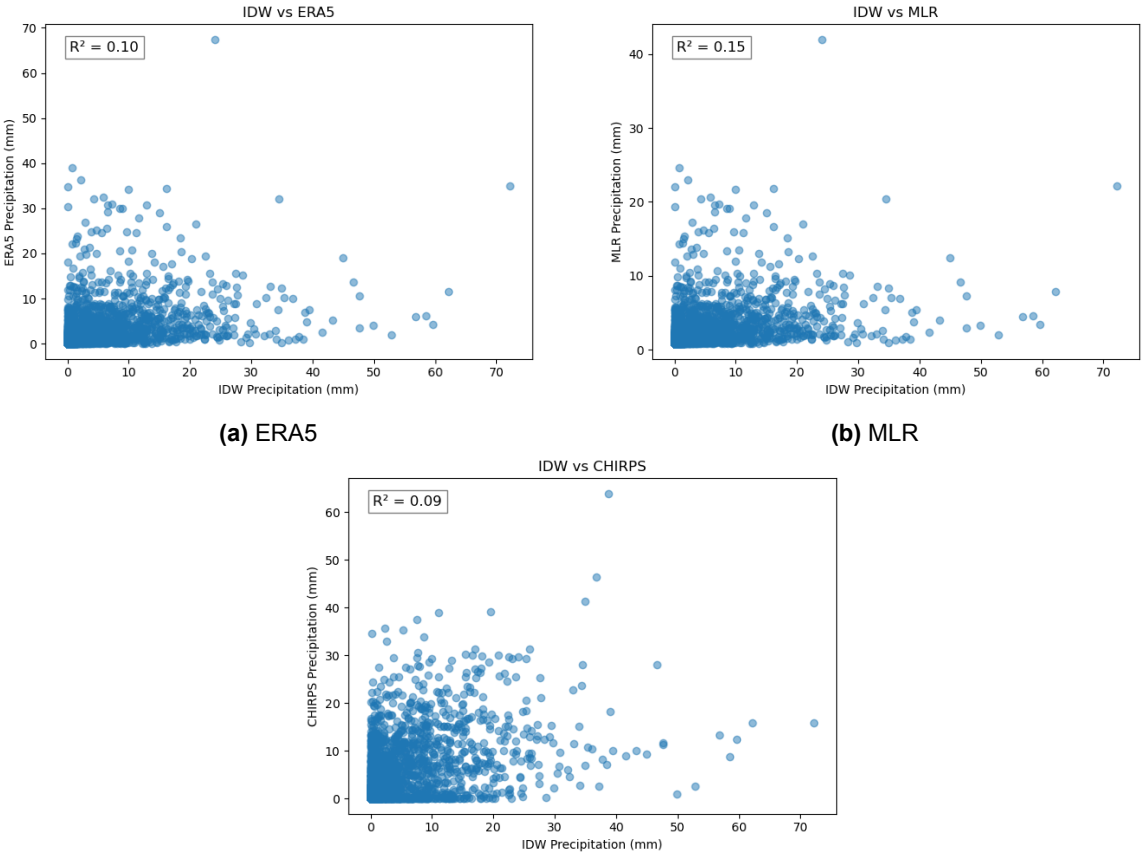

(a) ERA5

(b) MLR

(c) CHIRPS

Figure 4.7: Scatter plot of daily gauge precipitation interpolated using IDW versus (a) ERA5; (b) MLR; (c) CHIRPS for the entire period

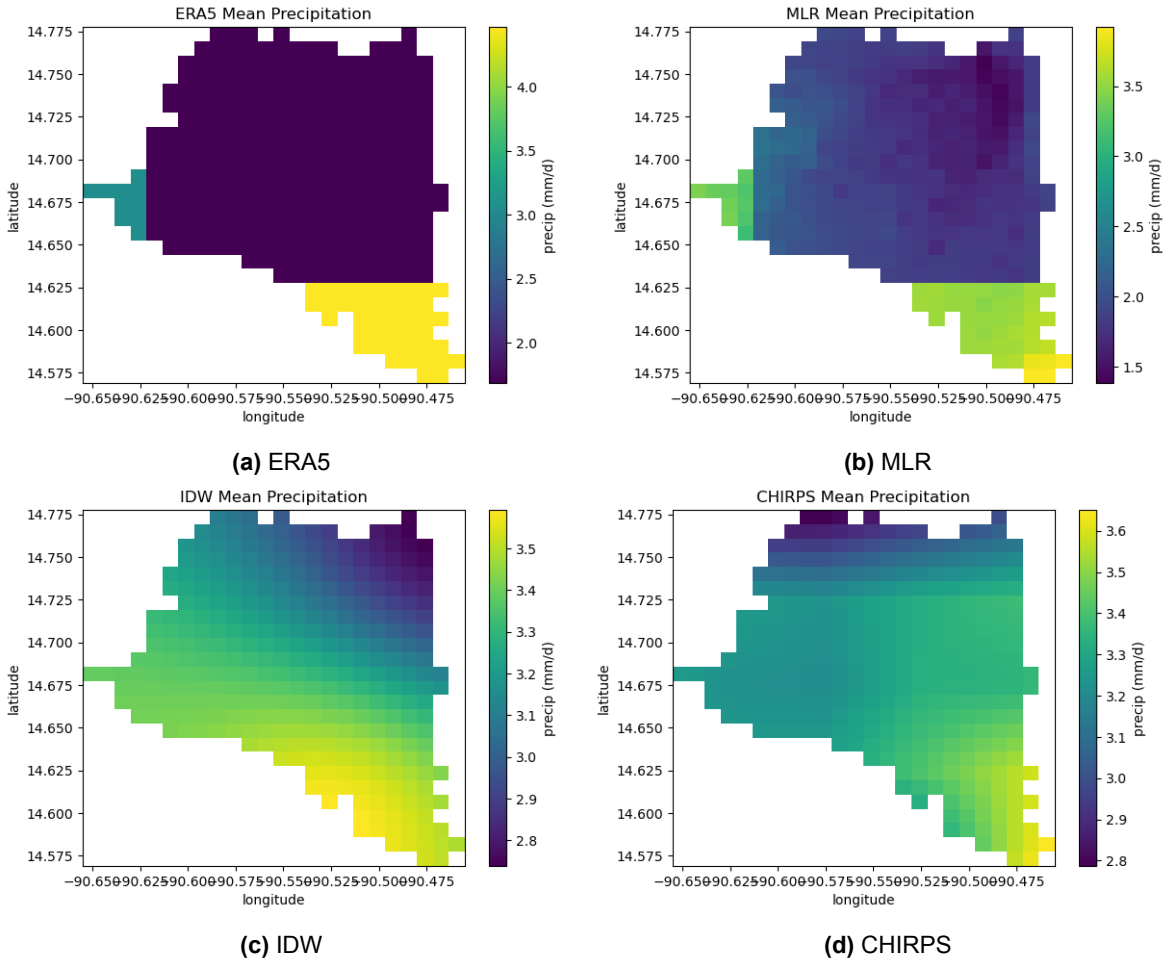

(a) ERA5 **(b)** MLR

(c) IDW **(d)** CHIRPS

Figure 4.8: The mean precipitation (2011-2019) from the different dataset in mm/d

4.3. Hydrological model

In this section, the hydrological model results are discussed. First, the base model and statistics are described. Second, the overall results are discussed, mainly focusing on the performance score. Subsequently, the yearly results of both models are presented, focusing on differences in anomalies with the observed discharge and the timing of the peaks.

4.3.1. Base model data

The base wflow model used for this study is the existing wflow model provided by Witteveen+Bos. The model was constructed using mainly globally available data. Then, several of these data were reanalysed and compiled into a wflow model. The data sources for building the wflow model are presented in Table **4.2**. The wflow model produced has the statistics presented in Table **4.3**.

Table 4.2: data sources used to construct the wflow model

Type	Source	Function
Landuse	GlobCover	Determine landuse classes
Landuse	modis_lai	Generate cyclic LAI parameter maps
Meteo	chelsa	Discharge estimate to determine river width
Meteo	ERA5	Forcing data: precipitation, temperature, potential evaporation (based on De Bruin method)
Meteo	era5_orography	Lapse correction, based on higher resolution DEM
Meteo	koppen_geiger	Discharge estimate to determine river width
Soil	soilgrids	Determine soil classes and related parameters
Topography	merit_hydro	Elevation model

Table 4.3: wflow model statistics

	Value	Unit
Catchment size	277.36	km2
Mean elevation	1522	m
Spatial resolution	0.00833	degree
Number of pixels	336	-
Model extent (lon)	-90.651, -90.459	degree
Model extent (lat)	14.573, 14.773	degree

4.3.2. Calibration

This section discusses the calibration and validation processes. During the calibration, it was found that the model cannot simulate the amount of baseflow as presented in Fig. **4.9a**. This aligns with the conclusion drawn from the hydrological characteristic (see Section **4.1**. Regarding hydrological characteristics, it was concluded that the baseflow is mainly the effect of human intervention in the form of wastewater effluent. Hence, a lateral inflow was introduced in the model to represent the city's wastewater effluent. However, the data on wastewater effluent and its dynamic is unavailable, resulting from the combination of wastewater effluent and natural baseflow. Therefore, it was deemed not wise to use the result of hydrograph separation as lateral inflow. To simplify the process, the wastewater effluent was assumed to be constant and calibrated using trial-and-error to determine the amount of wastewater discharge. The separation result was used as a guideline in this calibration process. Fig. **4.9** presents the simulation result by introducing the lateral inflow to the model. From this process, the lateral discharge of 3 m^3/s presents the best result and was used for the model. The final calibrated parameters of the wflow model are presented in Table **4.4**.

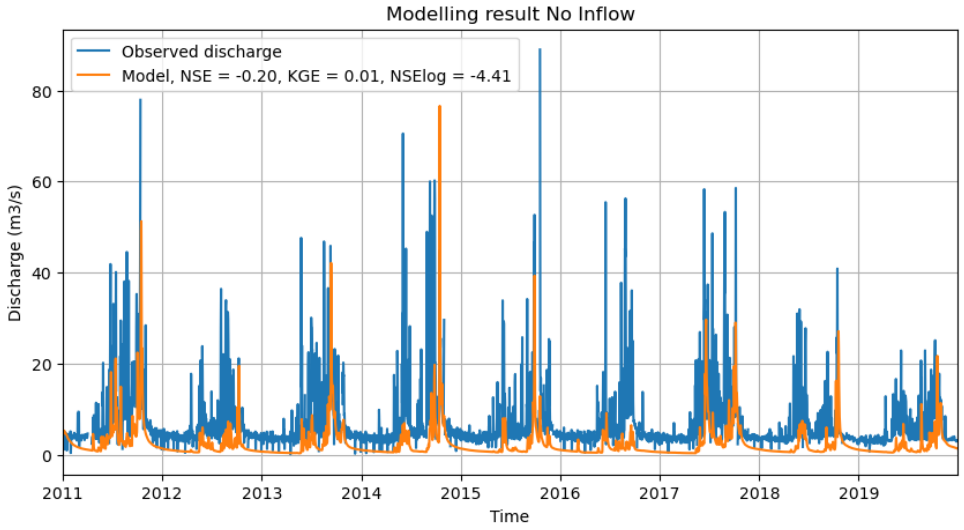

(a) Base model

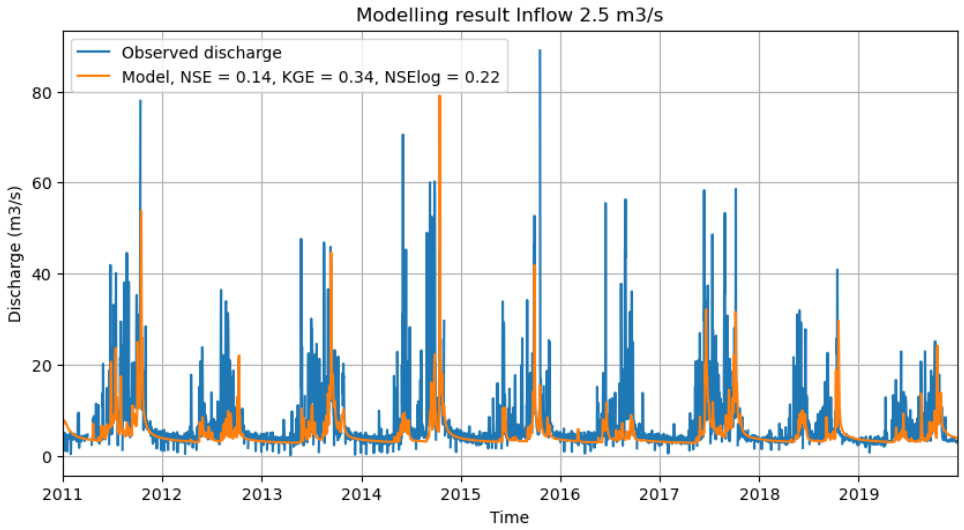

(b) Inflow 2.5 m^3/s

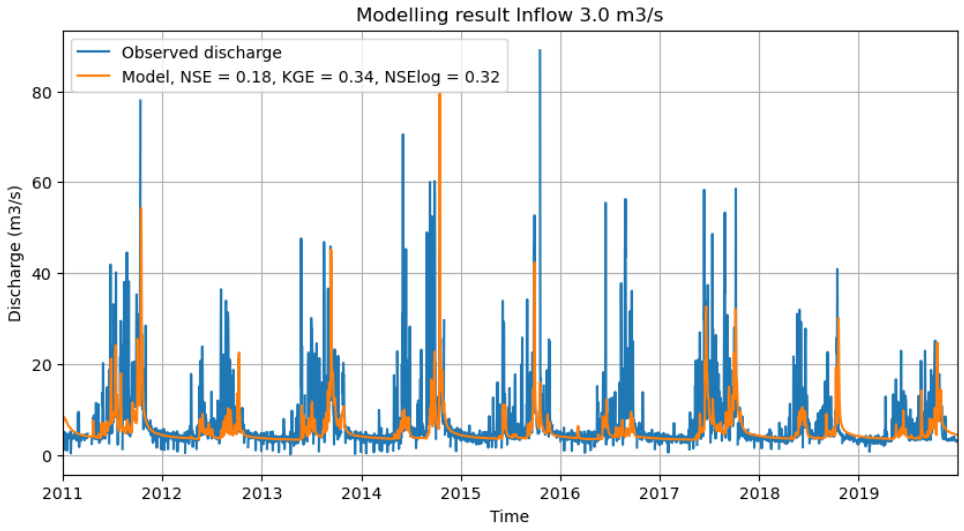

(c) Inflow 3.0 m^3/s

Figure 4.9: Comparison of the amount of lateral inflow introduced to the model and the effect on the performance score

Table 4.4: The final calibrated parameters for wflow model

Parameter	Base Value	Unit	Base Scale	Calibrated Scale
KsatVer	65.65 - 624.11	mm/d	1.0	5.0
KsatHorFrac	100	(-)	1.0	5.0
f	6.49E-4 - 1.73E-3	mm^{-1}	1.0	2.5
N	0.011 - 0.458	$s.m^{\frac{1}{3}}$	1.0	1.0
N_river	0.03 - 0.05	$s.m^{\frac{1}{3}}$	1.0	1.0
MaxLeakage	0	mm/d	1.0	1.0

4.3.3. Modelling result

First, the performance score of the discharge was considered, which offers a quantitative measure of the agreement between the model and the observed discharge, using the first and second years as a warm-up period. The hydrograph and corresponding performance score values are presented in Fig. **4.10**. The overall performance of the model was able to capture the bias and pattern of the observed streamflow with satisfactory results, presented by the KGE result > 0.3 for all precipitation forcing. However, the model was unable to get a reasonable estimate of the peak magnitude and timing of the streamflow, presented by no NSE result > 0.5. The NSE_{log} result was negligible because this study's low flow was synthesised using lateral inflow. The IDW shows the best result with KGE of 0.54 and NSE of 0.10, followed by CHIRPS and ERA5.

In addition to the performance score, this study also reports the cumulative flow. Table **4.5** displays the cumulative discharge over the period. The result varied over the years, but the IDW result aligns the closest to the observed cumulative discharge overall. However, the observed discharge has several missing data over the year that must be considered.

Table 4.5: The cumulative discharge per year (in mm)

Year	Observed	ERA5	IDW	CHIRPS
2011	915	1.090	1.200	1.223
2012	698	691	660	740
2013	808	924	828	949
2014	920	926	696	961
2015	753	760	705	716
2016	732	600	589	668
2017	900	1.004	768	768
2018	647	753	605	656
2019	641	743	876	830
Total	7.014	7.491	6.927	7.511

Yearly anomalies and model performance

Fig. **4.10** shows the result of the wflow model in one long time series. The detail per year is presented in Appendix **A**. Based on the figure, the following anomalies draw attention.

- **Year 2013:** The model is able to simulate the precipitation event. The CHIRPS dataset shows overestimation due to the fact that the dataset recorded more precipitation events at the smaller grid size. This contrasts with the ERA5 data, which shows a severe overestimation of peak discharge

in October. The phenomenon occurs due to the high precipitation event in the ERA5-dataset grid that covers a major share of the catchment, causing an extensive peak discharge. The IDW predicts underestimated discharge most of the time compared to the other dataset. However, the timing of the IDW agrees the best with the measurement data compared to other datasets, presented by the highest NSE score.

- **Year 2014:** In this hydrological year, ERA5 underestimates the peak discharge events throughout the year except one in October, which severely overestimates it. The disadvantages of ERA5's grid size are prominent this year because the grid that covers a major share of the catchment conforms better with the ground stations in the lower area. Hence, when the lower area of the catchment has intense precipitation events, in the model, it also propagates to the higher region, which is covered by urban areas. The CHIRPS and IDW datasets have comparable results, with the former performing better. The IDW dataset predicts an underestimated streamflow in October's precipitation event compared to CHIRPS.
- **Year 2015:** Generally, the model shows consistent underestimation of the measurement data as presented in Fig. **4.11**. The IDW shows the best result compared to other datasets in terms of timing. However, in terms of magnitude, the IDW dataset agrees with the measurement for the smaller peak (under 20 m^3/s) but underestimates the larger peak. This caused the IDW dataset to meet satisfactory results with NSE > 0.5 and KGE > 0.3 this year. The other two datasets also achieve an acceptable outcome regarding bias and patterns in the catchment, presented by KGE > 0.3. However, for the peak magnitudes, CHIRPS and ERA5 show an underestimation most of the time, with ERA5 lower than CHIRPS. ERA5 peak discharge presented in the previous two years also occurs this year.
- **Year 2016:** The anomaly presents in this year as presented in Fig. **4.12**. The model hardly agrees with the measurement. The model also underestimates whether per event or annual cumulative in this year. One of the causes is the sudden high peak in August, with no precipitation forcing response in the model. This occurrence could happen for two reasons: (1) an error in measurement discharge or (2) an extreme local convective storm that was not recorded in the precipitation forcing dataset. In several points, CHIRPS indicates an intense flood event in July and October, while other datasets did not. This also strengthens the hypotheses of the local convective storm in the middle of the catchment because, unlike the other dataset, CHIRPS has a finer grid and rainfall estimation.
- **Year 2017:** The same anomaly happened in 2016, also presents in 2017. The uniqueness of this year is the ERA5 dataset constantly predicts extreme flood events, while the other dataset did not predict anything. This occurrence was presented in June, September, and October events where the ERA5 predicted peak discharges. It contrasts with the 2016 event, where CHIRPS constantly predicted flood events while other data sets did not.
- **Year 2018:** The model result is not satisfactory. The model disagreed with the measurement, as the measurement recorded several flood events since the beginning of May, while the model only predicts after May. The KGE and NSE scores present poor results, especially for ERA5. ERA5 predicted an extreme flood event in October, which also occurred in 2013, 2014, and 2015. In the same event, CHIRPS managed to predict the event but severely underestimated the peak magnitude of the event. IDW, which also managed to predict the event and the peak magnitude, has off-timing.
- **the Year 2019:** In the model's final year, CHIRPS started very poorly indicated, with no events from May to July. Meanwhile, the other dataset agrees with the measured discharge, though having difficulties in predicting the peak magnitude. IDW and CHIRPS datasets also overestimated the flood

event from August to September. ERA5, despite underestimating the August-September flood event, overestimated one event in October when other datasets did not. This year's NSE and KGE scores are the poorest among others.

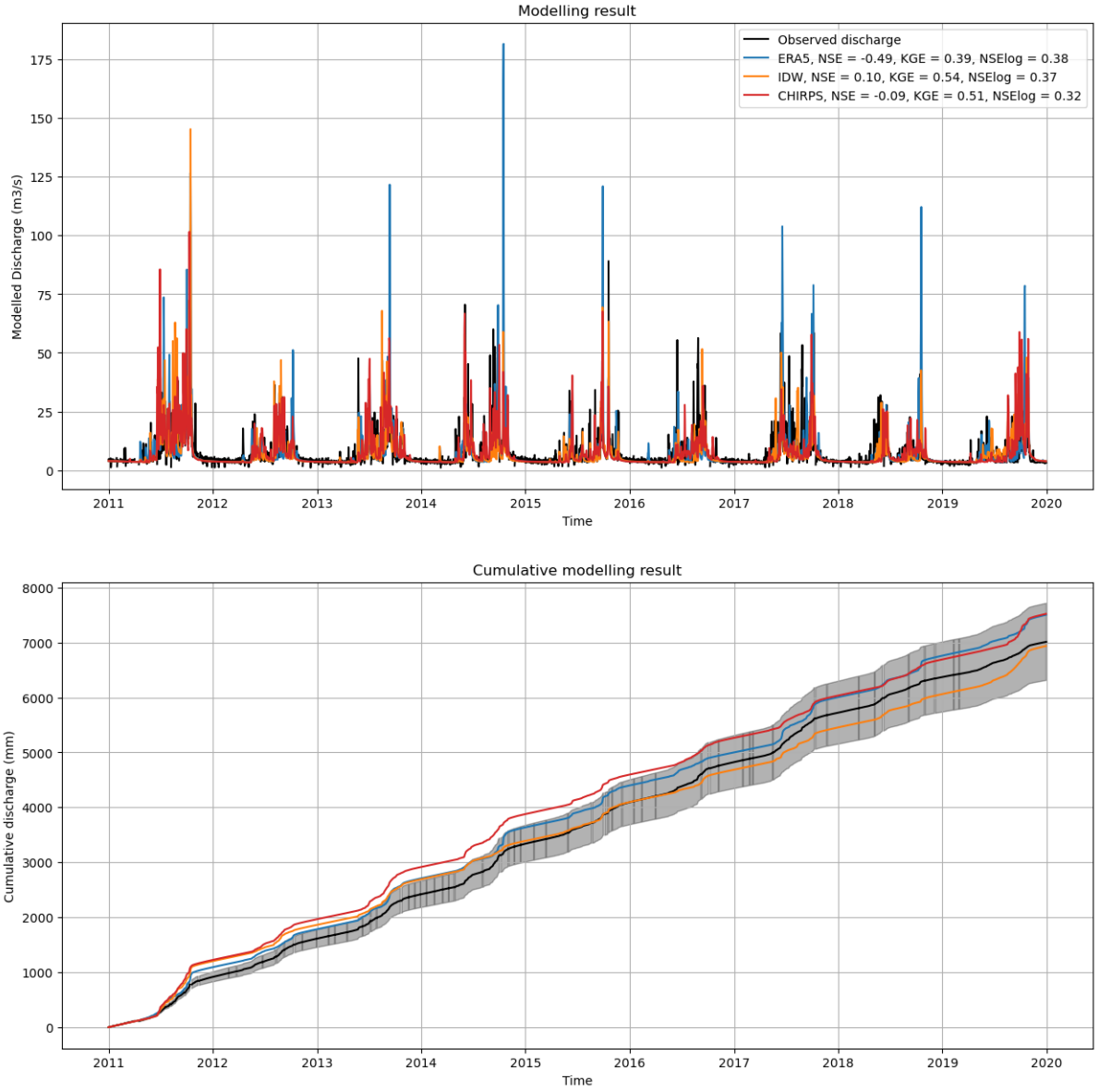

Figure 4.10: The long-term model result includes the cumulative discharge

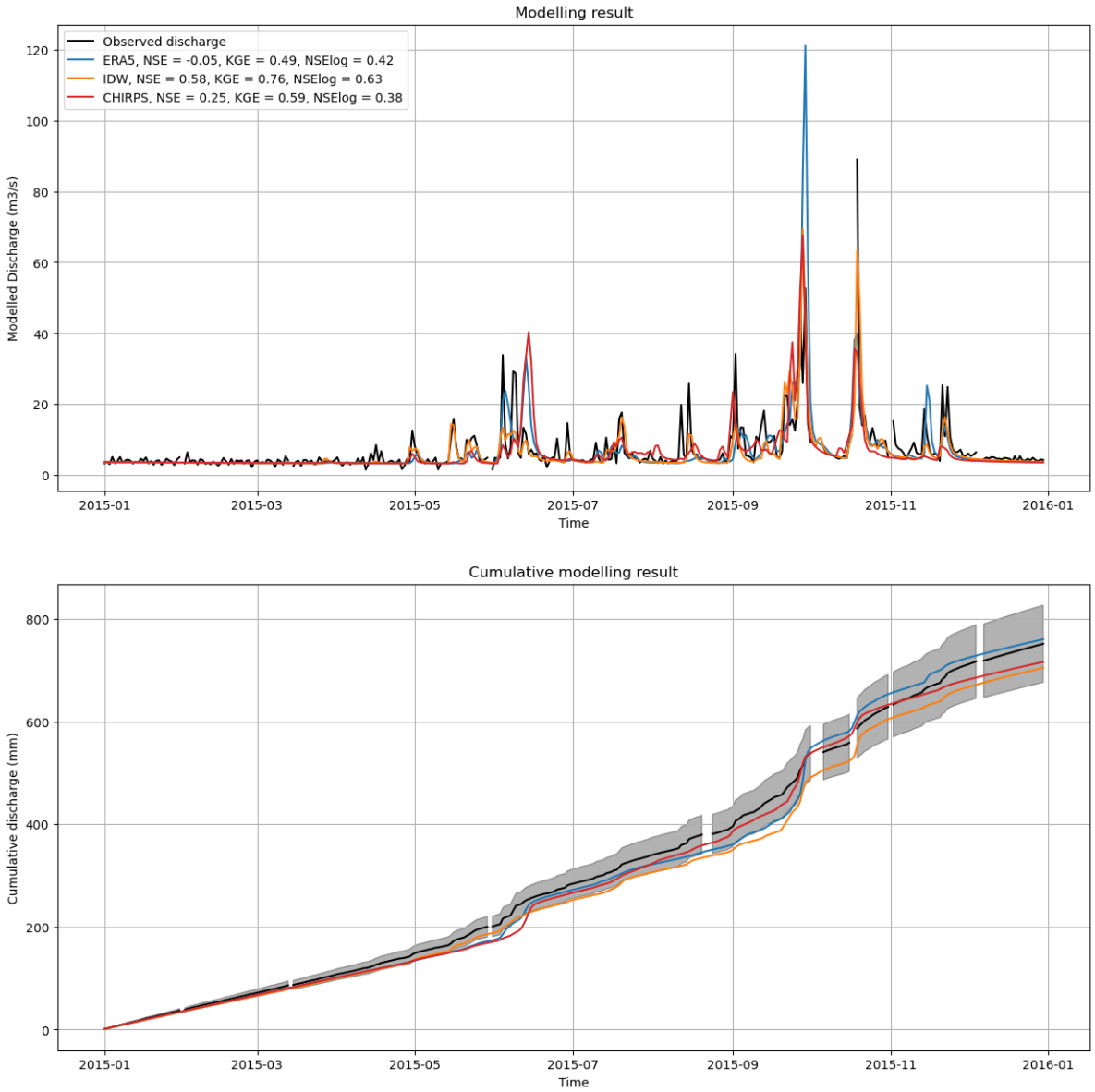

Figure 4.11: Modelling result Year 2015. This year shows the best model result compared to the other year. The IDW met satisfactory model condition with NSE > 0.5 and KGE > 0.3

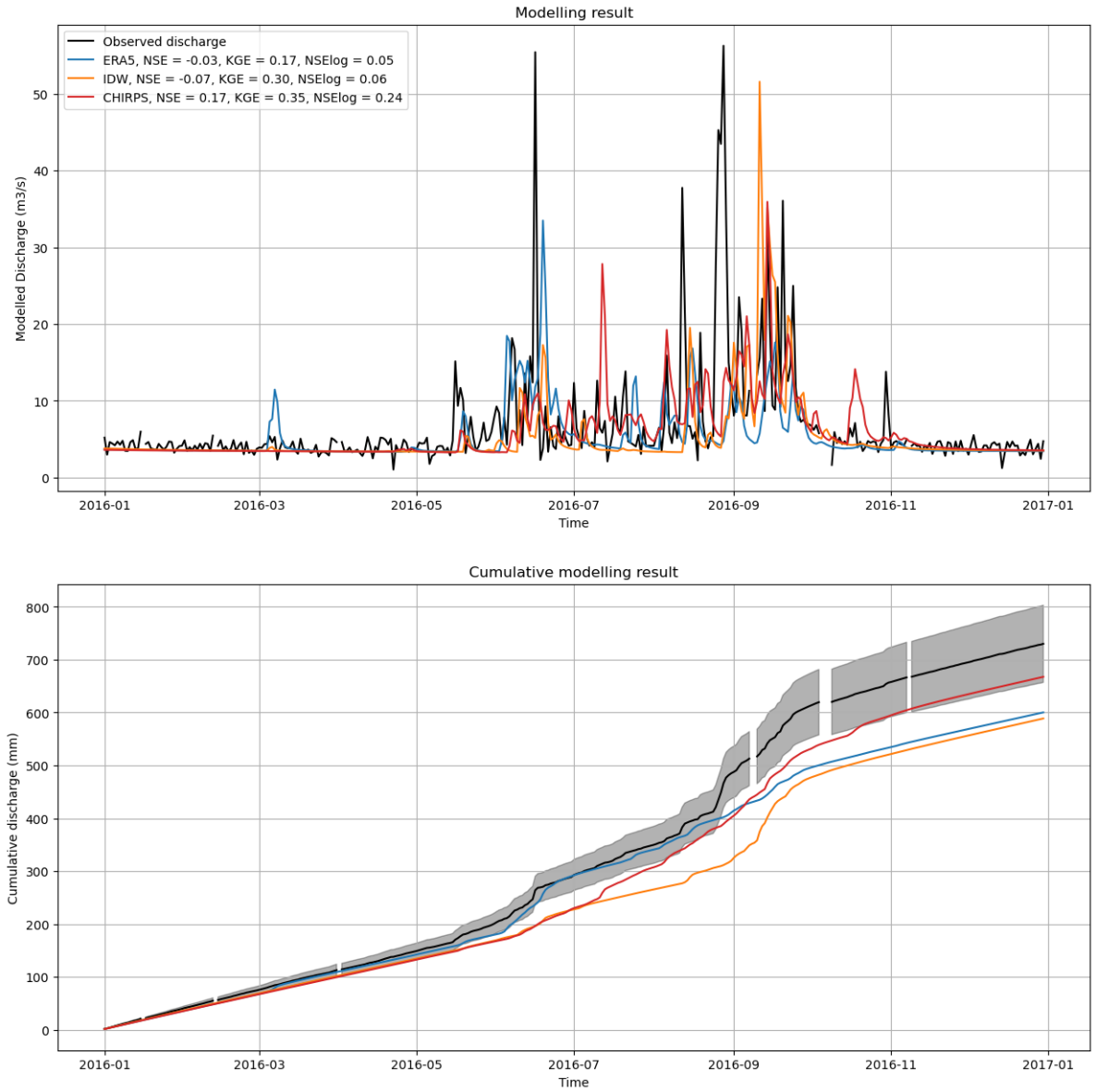

Figure 4.12: Modelling result Year 2016. This year starts the anomaly of either measurement or model results that persist to the following year. It presents that the three datasets disagreed with several flood events, notably CHIRPS, this year.

Impact of Spatially Distributed Precipitation

The distribution and variance of precipitation directly impact the result of runoff in each grid cell. Fig. **4.13** presents an example of the precipitation and the modelled runoff using wflow model on 02 September 2015. All three datasets show different spatial distributions, leading to varied distributed responses. In this period, ERA5 shows a comparable streamflow with IDW. However, this streamflow was mostly generated in the southern part of the catchment and did not show response in the urban areas (indicated in Latitude 14.6 - 14.7 degrees and Longitude -(90.525 - 90.600) degrees). The problem in IDW also propagates in the model result, as most of the runoff is generated in the southern part of the catchment. Overall, most of the streamflow was generated from runoff in urban areas, followed by arable lands. However, due to the size of ERA5's grid, the model often struggles to estimate a similar magnitude to the measurement discharge. On the other hand, IDW and CHIRPS provide better spatial distribution, and the model made a

better estimation compared to ERA5.

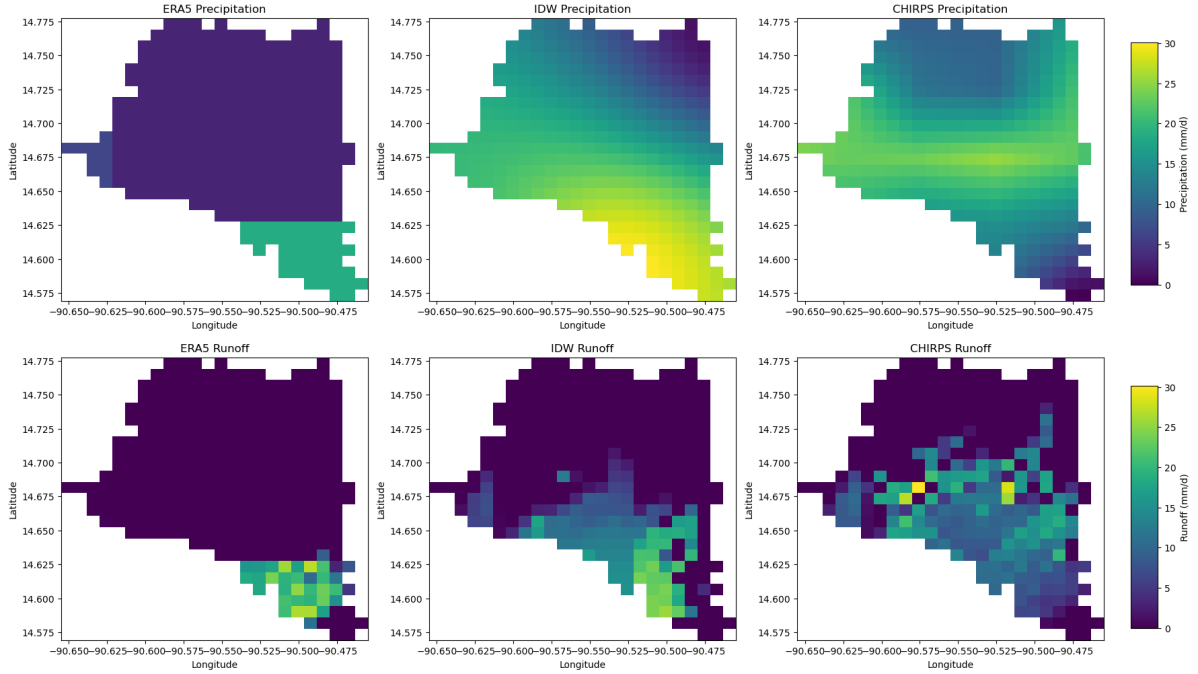

Figure 4.13: The spatial precipitation of each dataset and its corresponding modelled runoff result

4.3.4. Sensitivity Analysis

This section discussed several parameters that exert significant influence on the wflow model. The impact of these parameters will be delved into, including how they impact the model in timing, magnitude of peaks, cumulative discharge, and variations across different years. The sensitivity analysis was conducted manually on one extreme event in 2012

"Ksat" parameter

Ksat represents the hydraulic conductivity of the soil, which will affect the model's magnitude of peaks and baseflow. In wflow, Ksat is divided into two parameters, KsatHorFrac for the horizontal conductivity and KsatVer for the vertical conductivity. The initial value for KsatVer is derived from the soil data, while the KsatHorfrac assumes a default value of 100 mm/d. The KsatVer works on the vertical module, where the higher value means higher hydraulic conductivity, promoting more infiltration and reducing the magnitude of peak discharge. KsatHorFrac works on the lateral module, specifically on the subsurface flow, where the higher value supports interaction between the groundwater storage and streamflow. Hence, the higher value reduces the peak discharge magnitude, resulting in a milder recession. Due to its nature, KsatHorFrac can significantly influence the model performance because the initial value is not derived from the soil properties. Hence, having an expert guess on its magnitude can be challenging. Nevertheless, the range of hydraulic conductivity can be backed up by literature depending on the soil type, for example, Domenico et al., 1990 [13]. The sensitivity of Ksat parameters is presented in Fig. **4.14**

"f" parameter

This parameter represents the decay parameter of Ksat over the soil layer. The higher f value signifies a rapid decrease in Ksat with the soil depth, as presented in the blue line in the Fig. **4.15b**. This occurs because the soil's capability to conduct water diminishes rapidly, limiting the infiltration depth and increasing

the water volume that contributes to the overland flow. Fig. **4.15b** presents the effect of the f parameter on the Ksat decay over the soil thickness. The parameter itself did not differ much over varying scales as given in Fig. **4.15a**. Some jumps on minimal precipitation and a very high peak magnitude were demonstrated on the large scale of the f parameter. In contrast, the typical band of magnitude (scale of 0.1 - 10) did not show much variation in the simulated streamflow.

Other parameters

Other than the parameters discussed above, several other parameters were also inspected. The MaxLeakage parameter represents the maximum amount of water that can leave the model through deep groundwater flow. This parameter is also linked closely with KsatVer and f parameters due to the effect dependent on the amount of water circulating in the groundwater bucket. The impact of this parameter is not significant in this study because of the limited baseflow in the catchment. It is also hard to get an expert guess for the parameter, however, the ceiling for this parameter is 2 mm/day [27]. The Manning roughness of land and river cells was also inspected. Manning roughness represents the surface's roughness that is passed by the water flow and will affect the discharge timing. In the simulations carried out, this parameter affected not only the timing but also the peak's magnitude. This was understandable due to the catchment size and the model's timestep.

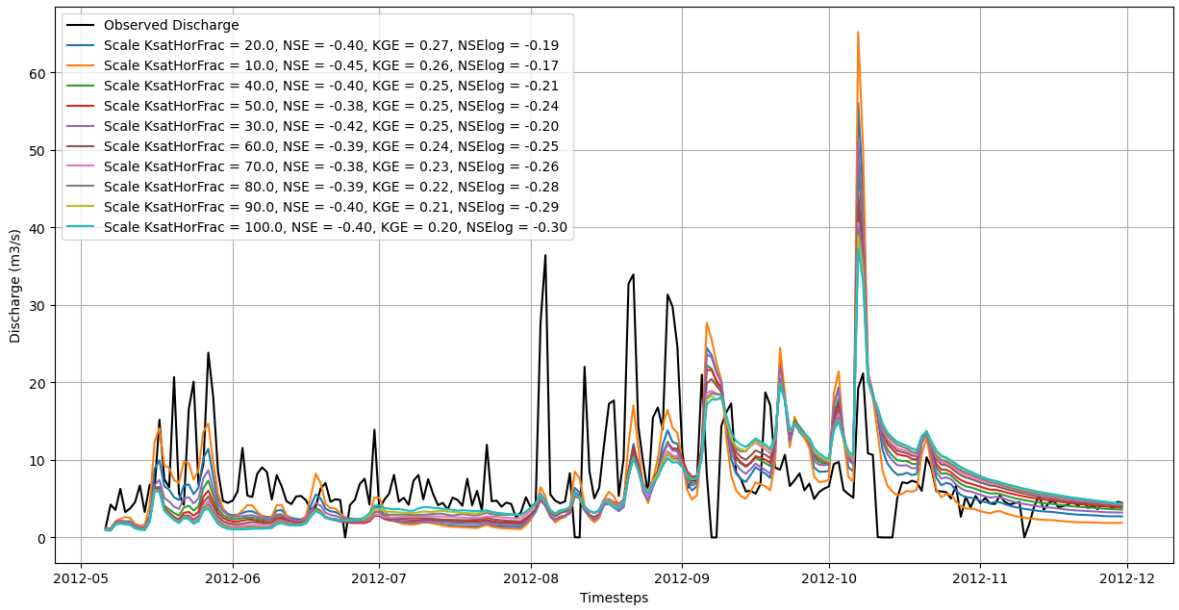

(a) KsatHorFrac

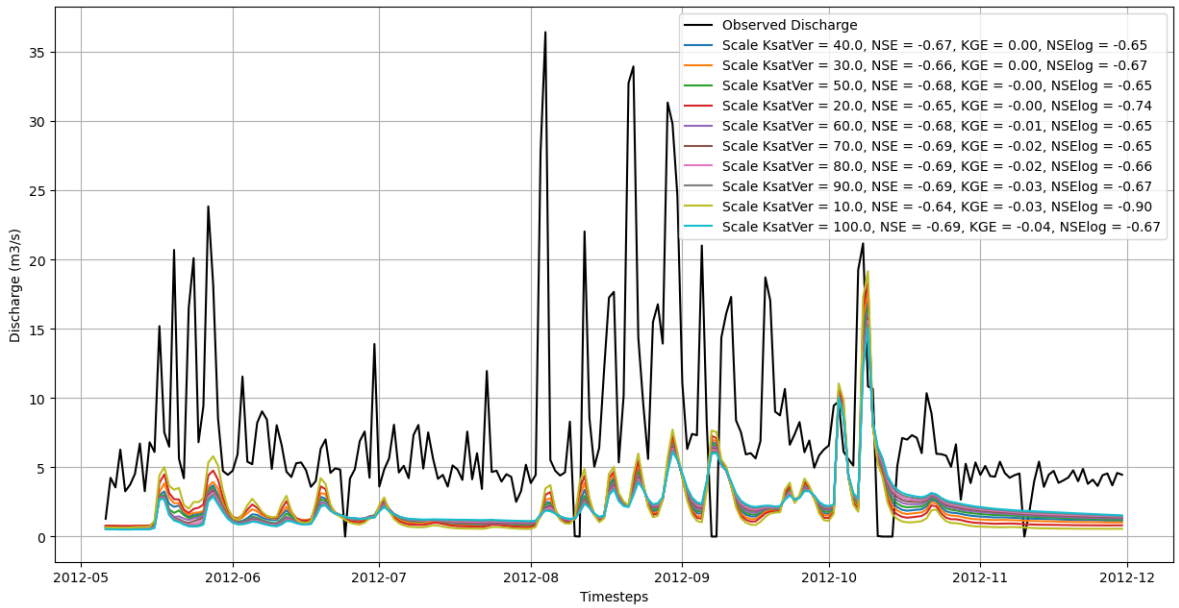

(b) KsatVer

Figure 4.14: Sensitivity of the Ksat parameter

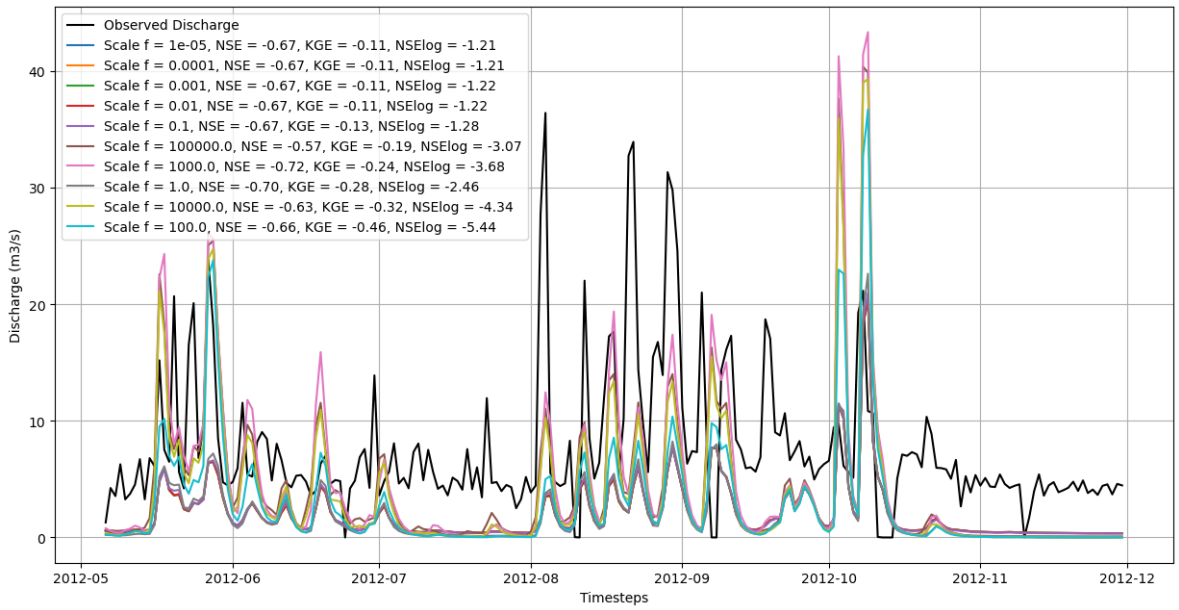

(a) Sensitivity of the f parameter

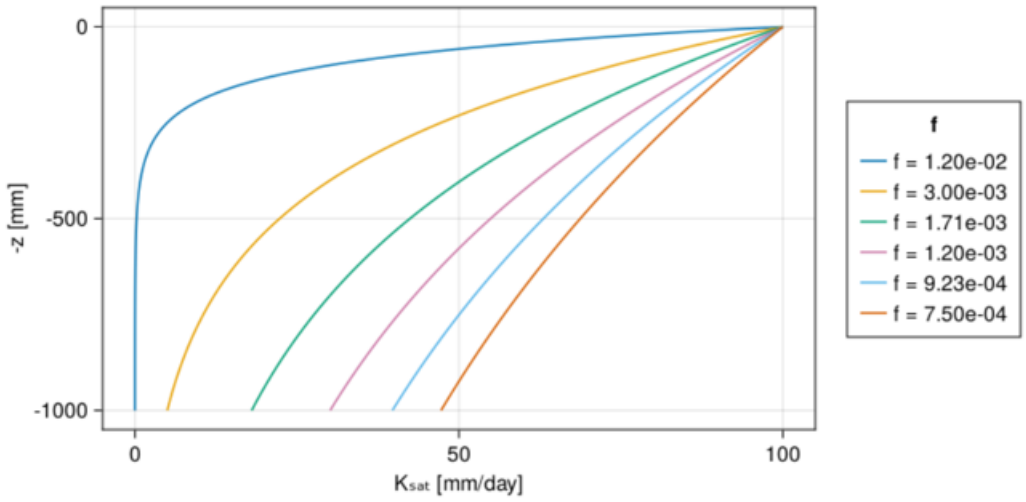

(b) Effect of f to KsatVer decay

Figure 4.15: (a) Sensitivity of the f parameter

5

Discussion

This chapter interprets the results and puts them into perspective. It first follows the same order as in the **Chapter 3** and **Chapter 4**.

5.1. Hydrological Characterisation

This section will discuss the findings during the data assessment and catchment profiling. Subsection **5.1.1** discussed the data refinement and the findings regarding precipitation data. Further, the pattern and hydrological processes behind the discharge data are delved in Subsection **5.1.2**. To summarise the characterisation, a simple water balance model was constructed, and the findings are presented in Subsection **5.1.3**

5.1.1. Precipitation

This section will discuss the precipitation used for this study. Limited access to the measurement data was a challenge at the beginning of the study. Most of the local measurements for this study were obtained as secondary data from previous research at Universidad del Valle, Guatemala, and the Aurora Airport station was obtained online.

Local measurements are often more accurate than satellite or reanalysis data because they directly measure precipitation without complex processing and calibration. However, local measurements pose disadvantages, such as time gaps and limited area coverage representation. The local measurement product also has a limitation of temporal coverage, mostly coming only in a daily value. The combination of these values and the actual quality of the local measurement data caused ascertained uncertainty.

As presented in Subsection **4.1.1**, all stations except Aurora Airport have consistent measurements. The higher amount of precipitation is slightly lean to the stations located in the higher area (Suiza Contenta and INSIVUMEH). The correlation-distance analysis showed a limited correlation between each station, especially between higher and lower altitudes stations. This indicated the precipitation predominantly by the small extent of convective storms, which was the reason for the discrepancies in the behaviour of each station. Hence, it proved the heterogeneity in spatial and temporal scales. The result from the correlation distance was further used to assess the station's network, assuming all stations work fine. The assessment shows the high variance and the error estimate from the available stations. The combination of heterogeneity, limited amount of ground stations, and no ground stations within the catchment became the factor of this high variance. This result led to the relative error estimate variance (Z_{areal}) found was very

high on the daily time series with an amount of 45%, exceeding the best practice's acceptance range of 5-10% [31, 12]. This indicates the network's error estimation to represent the precipitation in the catchment area. The absence of a rain gauge in the catchment's middle section also aggravated the network's misrepresentation. Thus, this finding highlights the uncertainty of the interpolation method. In addition, the analysis also estimates that the catchment required an additional 16 stations to have Z_{areal} under 10%.

5.1.2. Discharge

The Hidrovacas Dam operator owns discharge data. The discharge data is a relatively sensitive topic based on correspondence with Witteveen+Bos and the researcher from Universidad del Valle, Guatemala. Witteveen+Bos provided the water level of the dam reservoir, which was obtained from the dam operator. The discharge data of the river was also obtained as secondary data from the Universidad del Valle. The data from the university also claimed to be sourced from the dam operator and could not specify the exact location of the measurement. The correspondence with the university also found several identified interventions in the river stream, namely a mini hydro power plant upstream of the measurement location, effluent of wastewater from the wastewater treatment plant, and direct dumping from the households in Guatemala City and its vicinity. Later in the study, continuous correspondence effort resulted in additional hourly discharge data provided by Witteveen+Bos with time series from 2021 to 2022. It is difficult to compare the data from Universidad del Valle and Witteveen+Bos because the measurement times do not overlap. Nevertheless, a time-series comparison of the data from the university in 2019 and Witteveen+Bos in 2021 shows a similar baseflow magnitude. Hence, it was deduced that the measurement data was obtained from the same location.

Because of the limited options available to obtain the data, it is hard to deal with uncertainties. Nevertheless, the models must be calibrated using the available data. The facts mentioned above regarding the questionable measured discharge resulted in significant uncertainties in the hydrological model. As an alternative to obtain additional data, the spillway equation was used to obtain the reservoir outflow of the Hidrovacas Dam. However, the result obtained has a different magnitude compared to the streamflow data presented in Fig. **2.6**. The data is also not continuous because the reservoir outlet is human-controlled. Therefore, this study does not use the data derived from the spillway equation.

This study was based on data from the Universidad del Valle, and further verification was carried out to check the quality of the data. The data shows a lot of errors and noises (Fig. **2.6**). The low flow shows volatile changes and some values near zero in the graph. These near-zero values were assumed to have no data/error in measurement. The discharge pattern exhibits rapid changes, from almost no discharge to high discharge within a short period. The streamflow pattern also often did not correlate with the precipitation data. Therefore, it has been challenging on a digital low-pass filter. Usually, the digital low-pass filter uses the recession analysis to obtain the recession constant using the master recession curves method [25, 39, 14]. The sudden jumps and drops in the streamflow data presented brought a challenge during the analysis. Hence, this study used visual inspection after cleaning the data valued under 1 m^3/s, acknowledging disadvantages such as the inspector's subjectivity and uncertainty [59]. Nevertheless, this assumption was understandable since the analysis aimed to determine the characteristics and pattern instead of obtaining a definite value. The focal point of the inspection fitted the slope after the inflection point in the recession limb of the hydrograph.

The result was that the digital filter was well-fitted for the dry seasons of 2014 and 2017. However, in the other years, the slope of the baseflow separated using the digital filter was not fitted due to the slope of the recession being too steep or almost nonexistent, as presented in the dry season of 2019. Consequently,

it was difficult to draw definitive conclusions from this result alone. Therefore, the result was accepted and integrated into the existing literature on the catchment area. The minimum and maximum baseflow discharge aligns with the range of 2 - 4 m^3/s during the dry season [5]. The stable baseflow during the dry season indicates the vast and active groundwater storage [39, 14]. However, the involvement of baseflow during the wet season did not indicate an active groundwater interaction; it suggests the streamflow in the catchment was driven by the rainfall-runoff response [39]. According to the DRR report, the wastewater effluent from the city also contributes to the streamflow of Rio Las Vacas [5]; this is also strengthened by faecal matters in water puddles downstream of the city [23]. It is inconclusive to deduct the source of the baseflow in the catchment. Hence, a further water balance analysis was conducted to help characterise the Rio Las Vacas catchment.

5.1.3. Water Balance

The water balance analysis was conducted to conclude the hydrological characterisation of the catchment. The water balance was constructed using the ERA5 dataset. This decision was made due to limited evapotranspiration and meteorological data from other stations. The Aurora Airport ground station provided both precipitation and evaporation data. However, the quality of data in the Aurora Airport, which has inconsistencies and uncertainty, made this study decide not to use the data from the ground station.

The rainfall-runoff coefficient from the water balance was relatively high, around 0.4 - 0.6. Looking back at the catchment land cover and land usage, the coefficient seems attainable because of the growing urban areas and limited tree coverage in the catchment. However, the E_{act} obtained from a simple equation was far off compared to the E_{act} calculated from the theoretical Budyko framework. Meanwhile, the Budyko water balance showed that the catchment lacked precipitation to have the amount of discharge presented in the measurement. The discrepancy between the two methods assumed it was sourced from human intervention in the catchment. Budyko framework as an empirical approach overlooked the catchment's human intervention effect. The literature review and correspondence with local experts also clarified that the wastewater effluent from the city influenced the river discharge [5], but the magnitude of the influence was still unknown. Therefore, it was concluded that the baseflow of the catchment mainly came from the effect of wastewater effluent from the city. This conclusion was made based on the findings presented above and the hydrograph separation presented in the previous section, which showed a relatively steady baseflow, around 2 - 4 m^3/s during the dry season (between December and March). Furthermore, to strengthen this conclusion, a correction on discharge data by removing the wastewater effluent using the hydrograph separation result showed the evaporative index on a similar magnitude to the Budyko framework. The validation from the Budyko framework strengthens the assumption and shows the significance of human-induced changes in the catchment. These findings and conclusions regarding the catchment were carried out as input and consideration for the hydrological modelling.

5.2. Spatially Distributed Precipitation

Two interpolation methods were employed to create spatial coverage for these stations. The first one was using IDW. Since the gauge locations are relatively close (< 30 km) to each other and located at the edges of the catchment area, the value over the edges resembles the measurement values. The critical part was the middle section of the catchment, where the values from the three gauges meet. There was no local measurement around the area to validate the value obtained from IDW. A cross-validation to validate the result was also impossible because of the limited number of gauges. The second method was MLR. This method employs the DEM characteristics (longitude, latitude, and altitude) in the precipitation

estimation equation. The parameters for the equation were estimated using the MCMC algorithm. The result of monthly precipitation was considered good, with an acceptable average performance score (> 0.7). However, this result did not translate well into the daily precipitation estimation. It was believed because of the daily variability from the local measurement. The local gauges have minimal rainfall during the dry season and a generous amount during the wet season—this variability averages down the result of this method. The input for daily timescale, in this case, ERA5, was unsuitable for this method for several reasons. First, because the ERA5 has a relatively large grid for the catchment, it hardly catches the temporal variance. In Fig. **4.3** shows that the ground stations have high temporal variability; the large grid could overlook this variability. Second, the ERA5 value often underestimates the precipitation within the catchment, especially in the middle section, which was mainly covered by one tile (see Fig. **4.8a** in purple).

The assessment of the dataset was then conducted by comparing all the datasets in terms of spatial and temporal distribution. The scatter plot of the daily precipitation shows a weak correlation to interpolated local rain gauge data using IDW. The low correlation between CHIRPS and IDW was presumably due to different temporal dynamics and the algorithm behind each dataset. This was because CHIRPS, despite using IDW method in the ground data correction, also utilise the reanalysis and satellite data. The widely dispersed cluster also indicates there are timing discrepancies between CHIRPS and IDW. Another probable reason was due to the limited rain gauge data, especially in the middle of the catchment. As presented in Fig. **4.7**, the CHIRPS dataset estimates precipitation in the middle of the catchment (latitude 14.650 to 14.725 degrees), which was very different to the IDW estimate. This was because IDW spatial distribution depends on the local rain gauge as the input. The fact that no rain gauge data in the middle section made the IDW distribution in the middle only an average of the rain gauge networks. Meanwhile, for ERA5 and IDW, the low correlation was because of the less spatial distribution of ERA5, on top of the difference in the algorithm of these datasets. The majority of the catchment area was only covered by one ERA5 grid, compared to the more spatially varied IDW. The cluster formed between IDW and ERA5 was denser compared to the CHIRPS, which could indicate that the IDW and ERA5 have more agreement in the precipitation's timing compared to CHIRPS. For the MLR, all the results are similar to ERA5 since the dataset was used as the input behind the formula. The MLR result, though bringing improvement in the spatial variance of the precipitation, did not have much impact on improving ERA5 data. Hence, it was decided not to use the MLR result in the hydrologic model.

5.3. Hydrological modelling

This section delves into the hydrological model's results, from the sensitivity analysis to the final result. The sensitivity analysis, performed manually, initially started from a wide range of scales, and the result was used to narrow it down for the model calibration. The primary focus is identifying and discussing several parameters affecting the model performance.

The wflow model used was based on the SBM principle. The model contains a large number of parameters that provide flexibility in adjusting the model. However, the abundance of parameters also could lead to equifinality, which became a challenge to determine whether the model performs well for the correct reasons or because some parameters offset other parameters, affecting the result.

This study shows the wflow model was able to simulate the hydrological response of the catchment, despite only configuring a few parameters. The selected parameters primarily influence the vertical module. The sensitivity analysis shows that the parameters in the vertical module, especially the soil water, are significant to the model result. The calibration of these few parameters also indicates that the global

parameterisation proposed by Imhoff et al., 2020 [27] was adequate and applicable for this region. However, a deeper look at other parameters, such as rooting depth and infiltration capacity, to enhance its connection to the physical realities.

The result consistently has a lag time of 1-2 timestep from the measured discharge. This was understandable due to the nature of the catchment, which has a rapid response that could be less than a day [**TOC4Guatemala**, 17, 5]. Meanwhile, because of limited data, the best model that this study can produce was in a daily timescale, which might miss the fluctuation that happens hourly.

Lastly, although the result still did not satisfy the condition to be used for forecasting, the model was capable of capturing the hydrological signatures recorded in the measurement data. From this onwards, the study delved into how the forcing data affects the modelling result.

5.3.1. Comparing precipitation forcing data

The model's forcing input was changed while the model parameters remained unchanged to investigate the effect of spatial and temporal variability in precipitation. This study tested three types of forcing precipitation: ERA5, CHIRPS, and the ground stations interpolated using IDW. Performance scoring, cumulative discharge, and inspection were used to determine the performance of each forcing data set in the model.

Overall, the model could simulate floods in the catchment, especially during the wet season. There were no issues in the capability of the model to capture the bias and variability of the measurement, presented by the KGE > 0.3 for all models. However, none of the precipitation data met the satisfactory performance scoring, as shown by the lack of a model result with NSE > 0.5. The main issue with the model result was that it is incapable of predicting the peak magnitude and timing of the flood compared to the measurement. The NSE values are sensitive to offsets in timing and magnitude of the peaks, as discussed in Subsection **3.3.2**. The IDW showed better timing and discharge magnitude than the other forcing data, presented by the only positive NSE score despite poor performance. The validation scores show the difficulty of hydrological modelling in the data-scarce regions.

The cumulative discharge was not sensitive to the timing of peaks and, therefore, is a good value for validating the model. The gap in the measurement data made the cumulative discharge less reliable. However, this was still a good addition to the validation of the model. Overall, ERA5 and CHIRPS consistently overestimated the streamflow, while IDW slightly underestimated it. Considering the gaps in the measurement data due to error, the underestimation of IDW could be larger than reported, while the ERA5 and CHIRPS could be smaller.

In detail, looking over specific years, from 2013 to 2016, the model can simulate the streamflow compared to the measurement, with 2016 presenting the best result. However, from 2017 onwards, all forcing data struggled to predict a good result. The model often lacks response while measurement records a flood-level discharge. It became one of the uncertainties whether the model's errors in prediction or measurement errors.

Regarding the performance of forcing data, the ERA5 has the lowest scores among other data. In the year-by-year outlook, ERA5 consistently overestimate the flood event around November. This was consistent with the surge of precipitation that has been a known error of ERA5 in the mountainous area [22]. It also showed the valuation of forcing's grid resolution to the model's outcome. IDW and CHIRPS predicted flood simultaneously; however, they did not severely overestimate as much as ERA5. The finer resolution of IDW and CHIRPS indicated that this flood event probably occurred due to intense local

convective rainfall. Meanwhile, ERA5's grid propagated this event to almost the whole catchment, causing a severe overestimation of the event. The result of this study aligned with the previous study, especially Hafizi et al., 2022 [21] due to similar topography, where the model using the ERA5 dataset struggled to perform for streamflow validation.

The spatial distribution of ERA5 also showed disadvantages when assessing the runoff distribution of the model. The result using the ERA5 dataset often presents an overestimation or underestimation, especially in urban areas. Besides the precipitation distribution, land use also has significance in the runoff generation. The most runoff was generated from urban land cover, followed by the arable lands. Runoff generation over urban land cover is important for water quality or plastic transmission because the urban areas generate a significant pollutant in the watershed [60]. The formula developed by Meijer et al., 2021 [40] also put significance on the precipitation and land use in determining the probability of plastic transmission. The use of the ERA5 dataset for pollutant study in this catchment could diminish or magnify the effect of the hotspots located in urban areas. Hence, CHIRPS and IDW are considered better options for pollutant study.

In conclusion, considering the validation scores, cumulative discharge and spatial distribution, IDW is the best-performing forcing data. However, the lack of rain gauges inside the catchment caused the IDW dataset to overlook certain local rainfall that was not recorded in the available rain gauges. It made IDW, though the best performers, require certain conditions to perform, such as minimal local rainfall events in the middle of the catchment. Compared to CHIRPS, which responded to the majority of flood events measured, it shows that the data is not specialised for certain circumstances. IDW also underestimate the cumulative discharge. Considering the measurement discharge has missing data due to errors, the IDW underestimation could be more significant than reported. Furthermore, CHIRPS is one of the well-known datasets for hydrology study and has been used in the region [37]. In consideration of the aspects above, CHIRPS shows more promising results despite average scores.

5.3.2. Validation

It is hard to validate the result based on the performance scoring alone, especially the NSE and NSE_{log}. NSE and NSE_{log} metrics rely heavily on goodness-of-fit, which necessitates the alignment of timing and peak magnitude. However, due to the rapid response of catchment areas, achieving suitable timing in daily hydrological models is particularly challenging. Therefore, the utilisation of KGE is warranted. Unlike NSE and NSE_{log}, KGE evaluates the timing and peak magnitude and considers bias pattern and variability in model outcomes. This provides a more comprehensive assessment, especially in rapid-response catchment areas. However, the bias patterns and variability in KGE could overwhelm the peak magnitude and timing [33]. Therefore, both scoring is evaluated independently. In addition to the performance scoring, visual inspection and cumulative discharge were inspected during validation to ensure the model result.

Overall, the validation shows the model's consistent performance, shown by minimal discrepancies between the calibration performance score and the cumulative discharge magnitude. This indicates that the model is not specialised for a specific event.

6

Conclusion and recommendation

6.1. Conclusion

This research aimed to improve the hydrological model in the Rio Las Vacas basin, with the spatial-temporal heterogeneity of precipitation in the area. To address this objective, three sub-questions were investigated.

SQ1: How to verify and validate the quality of the ground data? The data for this study faced challenges in both quantity and quality due to the limited number of meteorological stations in the Rio Las Vacas catchment. To address this, the study employed several validation methods. First, double mass analysis to verify the consistencies of the precipitation data, where only three of the four available stations have consistent data. Second, the correlation-distance analysis was conducted to check the correlation of each station. The result showed that each station has limited correlation, thus indicating the heterogeneity of the precipitation in the area. Third, network analysis was also carried out and shows the error estimate variance (Z_{areal}) of 45% and 7% on a daily and monthly basis, respectively. High Z_{areal} indicates the error variance of the station's network to represent the precipitation in the catchment. The absence of stations in the middle section of the catchment also aggravated the misrepresentation. The findings suggest that adding 16 more stations was necessary to achieve an acceptable error rate under 10%.

SQ2: How to select the appropriate precipitation forcing data for the model? This study evaluates three precipitation datasets: local ground stations, ERA5, and CHIRPS. Inverse Distance Weighting (IDW) interpolation was applied to the local rain gauge data to enhance the spatial representation of precipitation. During the evaluation, the ERA5 had three grids covering the study area, with one grid covering the majority of the area. Although the ERA5 has been widely used for hydrology studies, it could not represent the heterogeneity of precipitation in this area. Multi-linear regression (MLR), combining ground stations, DEM characteristics, and ERA5 data, was used to generate new gridded precipitation data.

The evaluation result found that each precipitation dataset has its own character. The IDW dataset was limited to ground data coverage, especially in the middle of the catchment. ERA5 dataset has good temporal coverage but poor spatial resolution. This made capturing the spatial variability and, subsequently, temporal variability challenging for ERA5. CHIRPS had a finer resolution than ERA5, thus offering additional spatial variance coverage for this study. Thus, it offered a balance between the spatial and temporal coverage for the catchment. The comparison and correlation of these datasets resulted in the elimination of the MLR dataset to be used for the hydrological study. The main reason was that the dataset was almost

identical to the ERA5, which was the input, and the algorithm did not offer any improvement for the ERA5 dataset.

SQ3: What is the hydrology characteristic of the Rio Las Vacas basin? The hydrological model of the catchment was based on knowledge of the catchment behaviour and available data. In this study, the characterisation relied mainly on the ERA5 dataset due to the complete coverage of precipitation and potential evaporation and discharge measurement data. The catchment exhibits abundant baseflow, but the baseflow pattern did not suggest significant groundwater storage. Water balance analysis using the P-Q method and the Budyko framework revealed low actual evaporation. Compared to the Budyko framework, the result showed that the actual evaporation was significantly higher, and the catchment should not have the amount of discharge presented in the measurement. By combining the information from prior studies on the catchment, such as the Dutch Risk Reduction report [5] and Funcagua report [17], the high baseflow of Rio Las Vacas was severely influenced by human intervention.

SQ4: Comparing precipitation dataset; which simulates the discharge the best? Three precipitation datasets were tested in this study. Quantitative and qualitative validation was conducted to determine the best precipitation dataset. Based on the quantitative result, the rain gauge network interpolated using IDW provided the best result. However, from the qualitative side, the use of the IDW dataset posed a significant uncertainty. CHIRPS, while second-best in quantitative validation, offered better qualitative reliability as an established global dataset, providing more consistent spatial coverage and has been tested in the region. Meanwhile, ERA5, despite being known as an established global dataset, lacked spatial distribution. This limitation made ERA5 less effective, especially in catchments like Rio Las Vacas with complex topography and variable rainfall patterns. Furthermore, spatial distribution had an effect on runoff generation at the pixel level and the transmission of pollutants. Hence, for hydrological model applications in a catchment like Rio Las Vacas, CHIRPS was more suitable because of the balance between spatial resolution and reliability.

In short, modelling the Rio Las Vacas Basin remained a challenge due to the uncertainty of the hydrological model in a data-scarce basin and low data quality, which drove this study to perform extensive verification and validation in each step. The hydrological characterisation helped to create a good foundation of assumption for the hydrological model. This study also showed the capabilities of wflow to simulate the hydrological response of the relatively small catchment. The wflow model was calibrated using a few selected parameters, while the base value was obtained using global parameterisation. Looking at the model performance, the global parameterisation was considered adequate for a basin like Rio Las Vacas. The vertical parameters, especially related to soil water accounting, were found to have a significant magnitude to the model result. Among various precipitation datasets, fine-grid size and spatio-temporal representation of the basin were important. The model based on ERA5 data was improved significantly by changing the precipitation data to one that has a finer grid and spatio-temporal representation. The spatiotemporal representation also propagated to the spatiotemporal distribution of the runoff, which was crucial for the flood and pollutant transmission study. Based on the quantitative and qualitative results, CHIRPS was considered the most suitable dataset among the datasets used in this study to improve the hydrological model.

6.2. Limitations and Recommendation

The first recommendation would be to focus on the data. This study shows how difficult to handle the spatial-temporal heterogeneity of the precipitation, not to mention the human-induced changes inside

the catchment. The most critical part was collecting the precipitation data in the middle section of the catchment since the current rain gauge used in the study already provides data for the edges of the catchment. However, the elevation begins to rise in the middle of the catchment. There are probabilities of orographic effects due to the topography of the area, which was overlooked by the study. Extra precipitation data collection is recommended to reduce the network's error estimate variance. Based on the analysis, an additional 16 stations can reduce the Z_{areal} under 10%, which is under the best practices' acceptance range of 5-10% [31, 12]. The placement of these stations should follow the guidelines from the World Meteorology Organisation (WMO) to obtain the best efficiency.

The study also overlooked the evaporation because of the limited number of local gauges with sufficient meteorological data. The evaporation in this study solely relied on the meteorological data provided by the ERA5 product, though the data was tried to be normalised based on the elevation. Furthermore, several study shows that temperature and evaporation have significant effects on the soil moisture content, which is also beneficial to be included in the calibration and fine-tuning of the model [21, 11]. Another look into how the evaporation could be varied along the spatial spectrum could be analysed.

In this study, only one dataset per input was considered. However, during the assessment, it was found that the two global datasets correlate to the ground data differently. CHIRPS correlate with the amount of precipitation in the basin but not the temporal dynamics. Meanwhile, ERA5 correlate better to the temporal dynamic but performs poorly on the amount of precipitation in the basin due to its grid size. A probabilistic data fusion model to achieve water balance closure proposed by Schoups and Nasseri, 2021 [51] has the potential to improve the current study.

The study employed a 1-day time step due to the data availability. Looking at the rapid response of the catchment, a shorter time step could be beneficial. The DRR Team Report show that the initial response of the catchment came within 3-6 hours after the precipitation [**TOC4Guatemala**, 5]. The 1-day time step surely overlooks this variation. This could be the reason why the model had a lag time of 1-2 time steps behind the measurement discharge.

The next recommendation is to conduct a site visit, especially on the data measurements, which could be beneficial and offer insight into the catchment. The site visit report provided by the Witteveen+Bos limits the environmental condition of the catchment area. Another addition from several reports offers insight into the human altercation in the catchment. However, these reports did not offer the details of each altercation, and the modeller had a limited understanding of translating reality into the model.

A more comprehensive site visit can also enhance Wflow's capabilities. This study limits its tested parameters due to its limited understanding of the catchment. This study calibrated the parameters Ksat and f based on the soil type in the site visit reports. Meanwhile, other parameters could be delved into, such as infiltration capacity, soil thickness, and residual water content. The study found that the soil water accounting scheme of wflow is significant in generating the runoff. Hence, these parameters are recommended to be explored further in the future study with additional understanding and information from the site visit.

References

[1] Arino, O. et al. *Global Land Cover Map for 2009 (GlobCover 2009)*. © European Space Agency (ESA) & Université catholique de Louvain (UCL). 2012. URL: https://doi.org/10.1594/PANGAEA.787668.

[2] Arora, M. et al. “Spatial distribution and seasonal variability of rainfall in a mountainous basin in the Himalayan region”. In: *Water Resources Management* 20.4 (Aug. 2006), pp. 489–508. DOI: 10.1007/s11269-006-8773-4.

[3] Becker, R. et al. “Spatially distributed model calibration of a highly managed hydrological system using remote sensing-derived ET data”. In: *Journal of Hydrology* 577 (Oct. 2019). DOI: 10.1016/j.jhydrol.2019.123944.

[4] Blume, T. et al. “Rainfall-runoff response, event-based runoff coefficients and hydrograph separation”. In: *Hydrological Sciences Journal* 52.5 (Oct. 2007), pp. 843–862. DOI: 10.1623/hysj.52.5.843.

[5] Breukelman, H. et al. “DRR-Team Mission Report Guatemala”. Status: Draft. Reference: DRR217GT04. Drafted by Hans Breukelman, Arend de Wilde, Arjan Braamskamp, Rutger Perdon. Checked by Amber Douma, November 18 2017. Approved by Arjan Braamskamp. Project name: Expert advice on dealing with pollution in the rivers Las Vacas and Motagua in the vicinity of Guatemala City, Guatemala. Nov. 2017.

[6] Budyko, M. I. *Climate and Life*. New York: Academic Press, 1974.

[7] Buishand, T. A. “Networks for Precipitation and Evaporation”. In: *Design Aspects of Hydrological Network*. Proceeding No. 35. TNO, 1986, pp. 69–79.

[8] Casado-Rodríguez, J. et al. “Hydrograph separation for tackling equifinality in conceptual hydrological models”. In: *Journal of Hydrology* 610 (July 2022). DOI: 10.1016/j.jhydrol.2022.127816.

[9] Chang, M. et al. “Objective double□mass analysis”. In: *Water Resources Research* 10.6 (1974), pp. 1123–1126. DOI: 10.1029/WR010i006p01123.

[10] De Bruin, H. “From Penman to Makkink”. In: *Proceedings and Information: TNO Committee on Hydrological Research N°39*. Ed. by J. Hooghart. Den Haag: The Netherlands Organization for Applied Scientific Research TNO, 1987, pp. 5–31.

[11] Dembele, M. et al. “Suitability of 17 gridded rainfall and temperature datasets for large-scale hydrological modelling in West Africa”. In: *Hydrology and Earth System Sciences* 24.11 (Nov. 2020), pp. 5379–5406. DOI: 10.5194/hess-24-5379-2020.

[12] DHV Consultants and Delft Hydraulics. *How to Review Monitoring Networks*. Training module from Technical Assistance Hydrology Project funded by World Bank and Government of The Netherlands, presented in New Delhi. Feb. 2022.

[13] Domenico, P. A. et al. *Physical and Chemical Hydrogeology*. Wiley, 1990.

[14] Eckhardt, K. “How to construct recursive digital filters for baseflow separation”. In: *Hydrological Processes* 19.2 (Feb. 2005), pp. 507–515. DOI: 10.1002/hyp.5675.

[15] Emmerik, T. van et al. “Hydrology as a Driver of Floating River Plastic Transport”. In: *Earth’s Future* 10.8 (Aug. 2022). DOI: 10.1029/2022EF002811.

[16] Food and Agriculture Organization of the United Nations. *Crop evapotranspiration guidelines for computing crop water requirements*. Rome, Italy: Food & Agriculture Organization of the United Nations (FAO), Mar. 2005.

[17] Fundación para la Conservación del Agua de la Región Metropolitana de Guatemala. *Informe del estado del agua de la Región Metropolitana de Guatemala 2022: el agua nos une*. Guatemala, 2022.

[18] Funk, C. et al. “The climate hazards infrared precipitation with stations—a new environmental record for monitoring extremes”. In: *Scientific Data* 2 (2015), p. 150066. DOI: 10.1038/sdata.2015.66. URL: https://doi.org/10.1038/sdata.2015.66.

[19] George H. Hargreaves et al. “Reference Crop Evapotranspiration from Temperature”. In: *Applied Engineering in Agriculture* 1.2 (1985), pp. 96–99. DOI: 10.13031/2013.26773.

[20] Gupta, H. V. et al. “On typical range, sensitivity, and normalization of Mean Squared Error and Nash-Sutcliffe Efficiency type metrics”. In: *Water Resources Research* 47.10 (2011). DOI: 10.1029/2011WR010962.

[21] Hafizi, H. et al. “Assessment of 13 Gridded Precipitation Datasets for Hydrological Modeling in a Mountainous Basin”. In: *Atmosphere* 13.1 (Jan. 2022). DOI: 10.3390/atmos13010143.

[22] Hersbach, H. et al. “ERA5 hourly data on single levels from 1940 to present”. In: *Copernicus Climate Change Service (C3S) Climate Data Store (CDS)* (2023). DOI: 10.24381/cds.adbb2d47 (Accessed on 01-009-2023).

[23] Houwelingen, J. van et al. “Backwater Impact Assessment”. Status: Final. Reference: 129635/22-008.239. Project: Fences in the Rio Las Vacas. June 2022.

[24] Hrachowitz, M. et al. *A decade of Predictions in Ungauged Basins (PUB)-a review*. 2013. DOI: 10.1080/02626667.2013.803183.

[25] Hrachowitz, M. et al. “Process consistency in models: The importance of system signatures, expert knowledge, and process complexity”. In: *Water Resources Research* 50.9 (2014), pp. 7445–7469. DOI: 10.1002/2014WR015484.

[26] Hrachowitz, M. et al. “HESS Opinions: The complementary merits of competing modelling philosophies in hydrology”. In: *Hydrology and Earth System Sciences* 21.8 (Aug. 2017), pp. 3953–3973. DOI: 10.5194/hess-21-3953-2017.

[27] Imhoff, R. O. et al. “Scaling Point-Scale (Pedo)transfer Functions to Seamless Large-Domain Parameter Estimates for High-Resolution Distributed Hydrologic Modeling: An Example for the Rhine River”. In: *Water Resources Research* 56.4 (2020), e2019WR026807. DOI: https://doi.org/10.1029/2019WR026807.

[28] Incer Nuñez, D. J. “Disponibilidad hídrica en la subcuenca del río Las Vacas utilizando el modelo Hydro-BID”. In: *Congreso Nacional de Recursos Hídricos 2023*. Guatemala, 2023.

[29] Jambeck, J. R. et al. “Plastic waste inputs from land into the ocean”. In: *Science* 347.6223 (Feb. 2015), pp. 764–768. DOI: 10.1126/science.1260879.

[30] Japan International Cooperation Agency (JICA). *The Study for Establishment of Base Maps and Hazard Maps for GIS in the Republic of Guatemala*. Report. rep. 2003.

[31] Kagan, R. “Precipitation - Statistical Principle”. In: *Casebook on Hydrological Network Design Practice*. Geneva, Switzerland: World Meteorological Organization, 1972.

[32] Kikaki, A. et al. “Remotely sensing the source and transport of marine plastic debris in Bay Islands of Honduras (Caribbean Sea)”. In: *Remote Sensing* 12.11 (June 2020). DOI: 10.3390/rs12111727.

[33] Knoben, W. J. M. et al. “Technical note: Inherent benchmark or not? Comparing Nash-Sutcliffe and Kling-Gupta efficiency scores”. In: (July 2019). DOI: 10.5194/hess-2019-327.

[34] Krause, P. et al. *Comparison of different efficiency criteria for hydrological model assessment*. Tech. rep. 2005, pp. 89–97.

[35] Lebreton, L. C. et al. “River plastic emissions to the world’s oceans”. In: *Nature Communications* 8 (June 2017). DOI: 10.1038/ncomms15611.

[36] Liu, J. et al. “Spatial Downscaling of TRMM Precipitation Data Using an Optimal Subset Regression Model with NDVI and Terrain Factors in the Yarlung Zangbo River Basin, China”. In: *Advances in Meteorology* 2018 (Mar. 2018), pp. 1–13. DOI: 10.1155/2018/3491960.

[37] López-Bermeo, C. et al. “Validation of the accuracy of the CHIRPS precipitation dataset at representing climate variability in a tropical mountainous region of South America”. In: *Physics and Chemistry of the Earth, Parts A/B/C* 127 (Oct. 2022), p. 103184. DOI: 10.1016/J.PCE.2022.103184.

[38] Ly, S. et al. *B A Different methods for spatial interpolation of rainfall data for operational hydrology and hydrological modeling at watershed scale. A review*. Tech. rep. 2. 2013, pp. 392–406.

[39] McMillan, H. “Linking hydrologic signatures to hydrologic processes: A review”. In: *Hydrological Processes* 34.6 (Mar. 2020), pp. 1393–1409. DOI: 10.1002/hyp.13632.

[40] Meijer, L. J. J. et al. *More than 1000 rivers account for 80% of global riverine plastic emissions into the ocean*. Tech. rep. 2021. URL: https://www.science.org.

[41] Moriasi, D. N. et al. “Model Evaluation Guidelines for Systematic Quantification of Accuracy in Watershed Simulations”. In: *Transactions of the ASABE* 50.3 (2007), pp. 885–900. DOI: 10.13031/2013.23153.

[42] *NASA Shuttle Radar Topography Mission (SRTM) (2013). Shuttle Radar Topography Mission (SRTM) Global. Distributed by OpenTopography.* https://doi.org/10.5069/G9445JDF. Accessed: 2023-10-12. 2013.

[43] Nash, J. E. et al. “River flow forecasting through conceptual models part I — A discussion of principles”. In: *Journal of Hydrology* 10.3 (Apr. 1970), pp. 282–290. DOI: 10.1016/0022-1694(70)90255-6.

[44] Obrist□Farner, J. et al. “Incoherency in Central American hydroclimate proxy records spanning the last millennium”. In: *Paleoceanography and Paleoclimatology* (Mar. 2023). DOI: 10.1029/2022pa004445.

[45] Pechlivanidis, I. et al. *Catchment scale hydrological modelling: A review of model types, calibration approaches and uncertainty analysis methods in the context of recent developments in technology and*

application. Tech. rep. 3. 2011, pp. 193–214. URL: https://www.researchgate.net/publication/266341273.

[46] Ranhao, S. et al. “A multivariate regression model for predicting precipitation in the Daqing Mountains”. In: *Mountain Research and Development* 28.3-4 (Aug. 2008), pp. 318–325. DOI: 10.1659/mrd.0944.

[47] Richts, A. et al. “WHYMAP and the Groundwater Resources Map of the World 1:25,000,000”. In: *Sustaining Groundwater Resources*. Springer Netherlands, 2011, pp. 159–173. DOI: 10.1007/978-90-481-3426-7_10.

[48] Roebroek, C. T. et al. “Plastic in global rivers: Are floods making it worse?” In: *Environmental Research Letters* 16.2 (Feb. 2021). DOI: 10.1088/1748-9326/abd5df.

[49] Schellekens, J. *wflow Documentation*. 2020.

[50] Schmidt, C. et al. “Export of Plastic Debris by Rivers into the Sea”. In: *Environmental Science and Technology* 51.21 (Nov. 2017), pp. 12246–12253. DOI: 10.1021/acs.est.7b02368.

[51] Schoups, G. et al. “GRACEfully Closing the Water Balance: A Data-Driven Probabilistic Approach Applied to River Basins in Iran”. In: *Water Resources Research* 57.6 (2021). Article e2020WR029071, pp. 1–27. DOI: 10.1029/2020WR029071.

[52] Segond, M. L. et al. “The significance of spatial rainfall representation for flood runoff estimation: A numerical evaluation based on the Lee catchment, UK”. In: *Journal of Hydrology* 347.1-2 (Dec. 2007), pp. 116–131. DOI: 10.1016/j.jhydrol.2007.09.040.

[53] Taheri, M. et al. “Localized linear regression methods for estimating monthly precipitation grids using elevation, rain gauge, and TRMM data”. In: *Theoretical and Applied Climatology* 142.1-2 (Oct. 2020), pp. 623–641. DOI: 10.1007/s00704-020-03320-2.

[54] Thattai, D. et al. *Hydrometeorology and Variability of Water Discharge and Sediment Load in the Inner Gulf of Honduras, Western Caribbean*. Tech. rep. 2003.

[55] US Army Corps of Engineers. *Water Resources Assessment of Guatemala*. June 2000.

[56] Villarini, G. et al. “Rainfall and sampling uncertainties: A rain gauge perspective”. In: *Journal of Geophysical Research Atmospheres* 113.11 (June 2008). DOI: 10.1029/2007JD009214.

[57] Wang, C. et al. “Advances in Hydrological Modelling with the Budyko Framework: A Review”. In: *Progress in Physical Geography* 40.3 (2016), pp. 409–430.

[58] Wannasin, C. et al. “Daily flow simulation in Thailand Part I: Testing a distributed hydrological model with seamless parameter maps based on global data”. In: *Journal of Hydrology: Regional Studies* 34 (2021), p. 100794. DOI: https://doi.org/10.1016/j.ejrh.2021.100794. URL: https://www.sciencedirect.com/science/article/pii/S2214581821000239.

[59] Willems, P. “A time series tool to support the multi-criteria performance evaluation of rainfall-runoff models”. In: *Environmental Modelling and Software* 24.3 (Mar. 2009), pp. 311–321. DOI: 10.1016/j.envsoft.2008.09.005.

[60] Windsor, F. M. et al. *A catchment-scale perspective of plastic pollution*. Apr. 2019. DOI: 10.1111/gcb.14572.

[61] Winsemius, H. C. et al. “On the calibration of hydrological models in ungauged basins: A framework for integrating hard and soft hydrological information”. In: *Water Resources Research* 45.1 (2009). DOI: 10.1029/2009WR007706.

[62] Witt, D. te. *Calibration of a wflow Model*. Internal memo of Witteveen+Bos. Sept. 2022.

[63] Yamazaki, D. et al. “MERIT Hydro: A High-Resolution Global Hydrography Map Based on Latest Topography Dataset”. In: *Water Resources Research* 55.6 (June 2019), pp. 5053–5073. DOI: 10.1029/2019WR024873.

[64] Zhang, L. et al. “Water balance modelling: concepts and applications”. In: *ACIAR Monograph Series* 84 (2002), pp. 31–47.

A

Figures: Modelling result each year

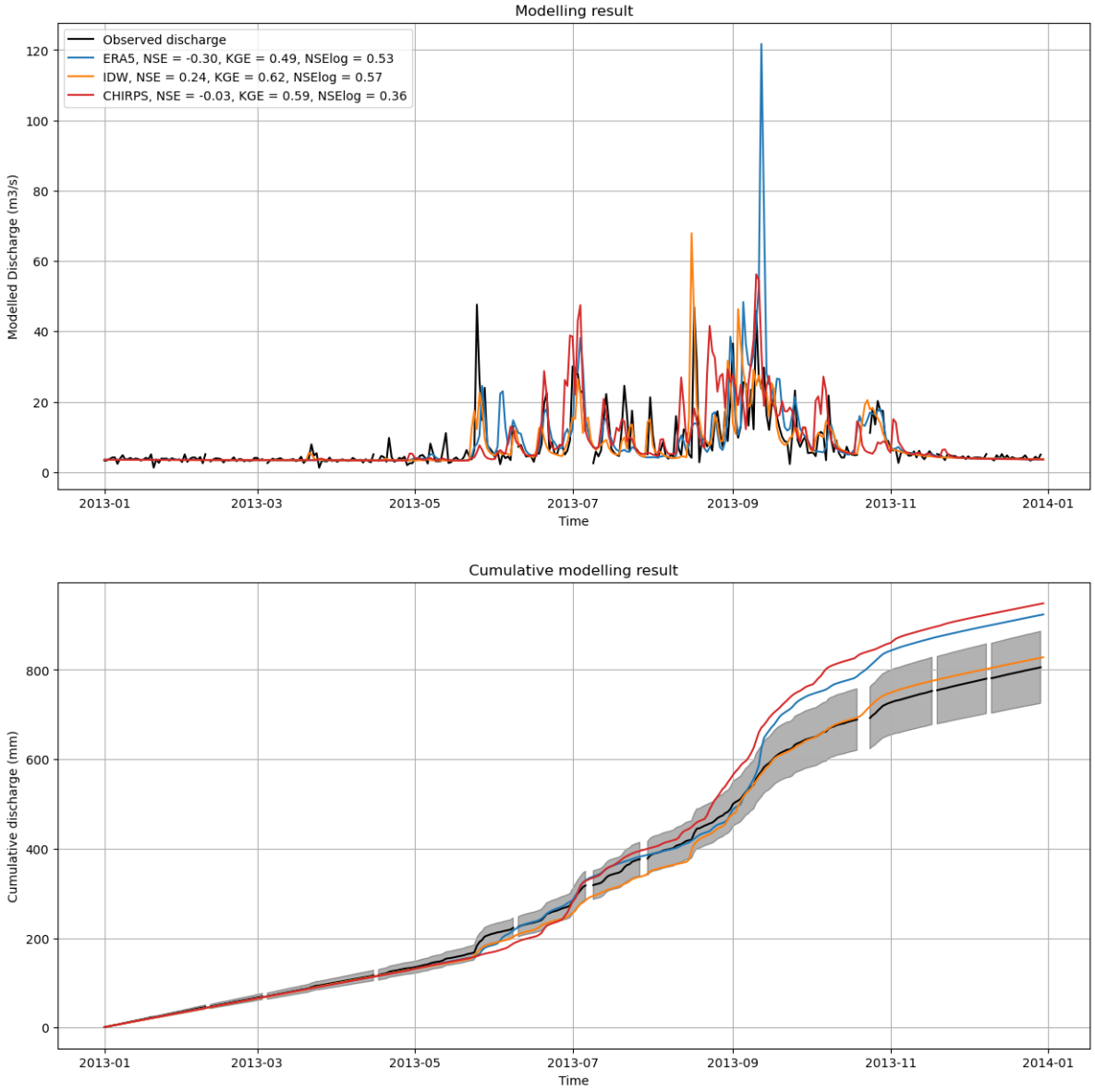

Figure A.1: Model run 2013

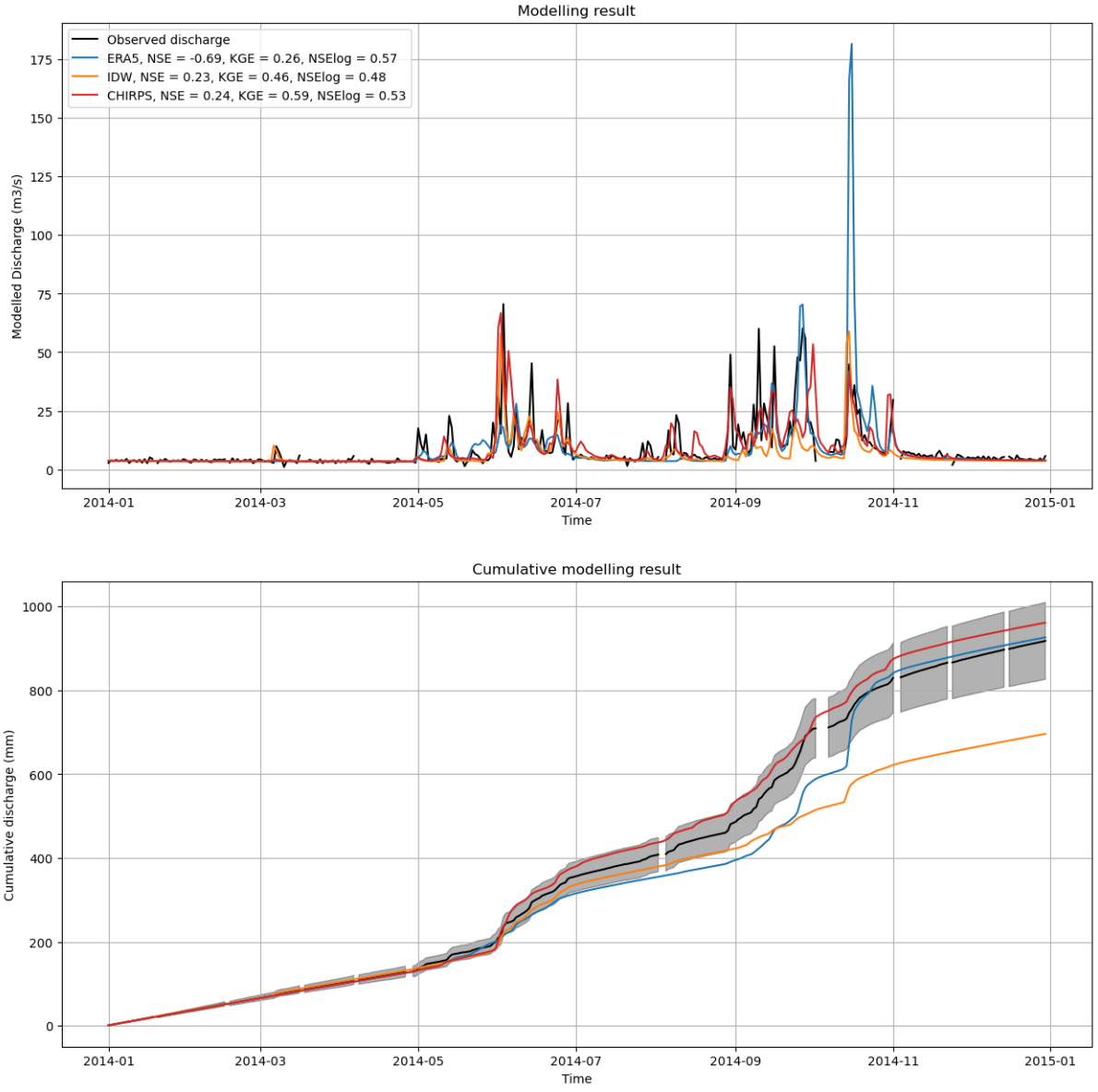

Figure A.2: Model run 2014

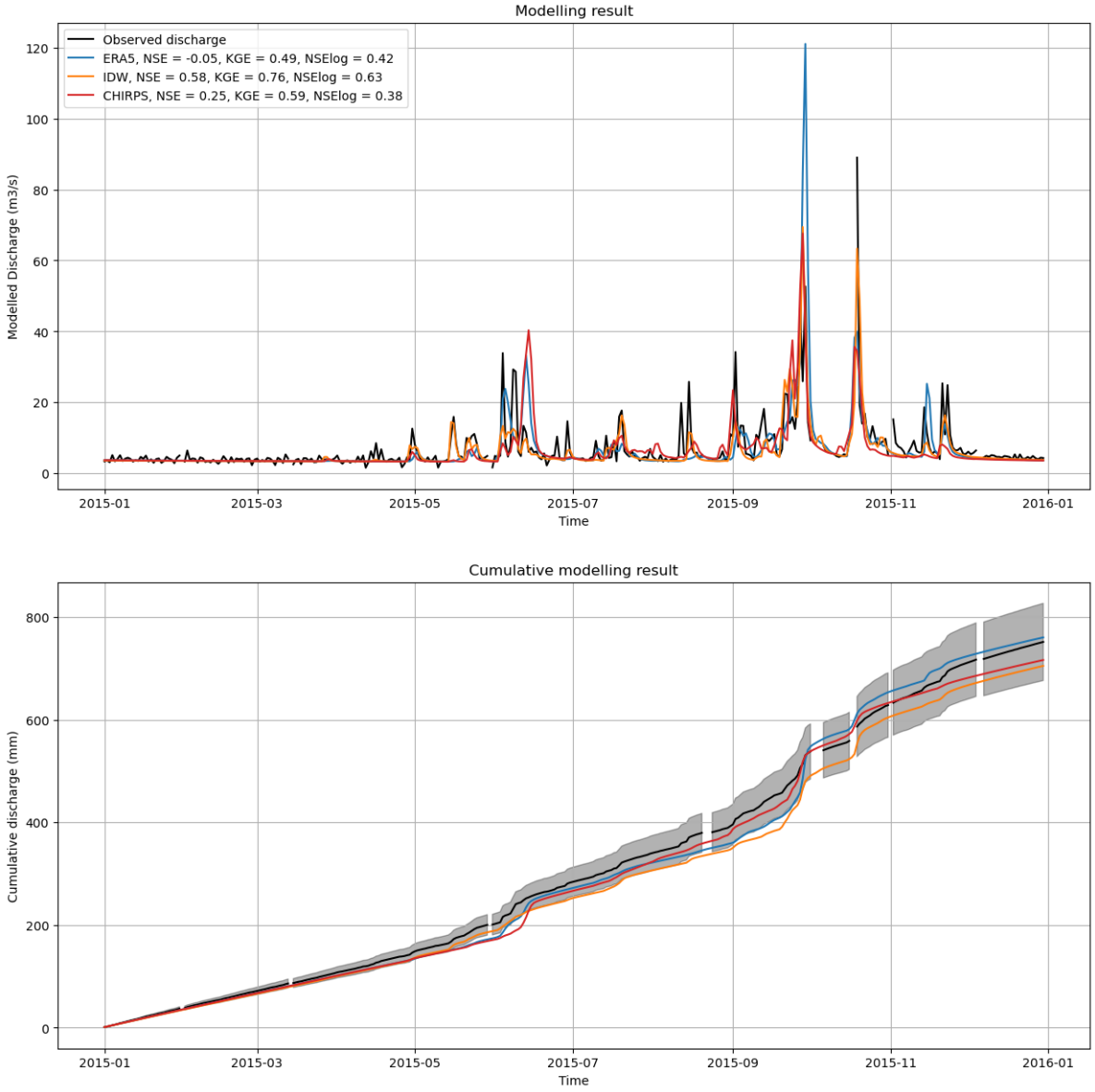

Figure A.3: Model run 2015

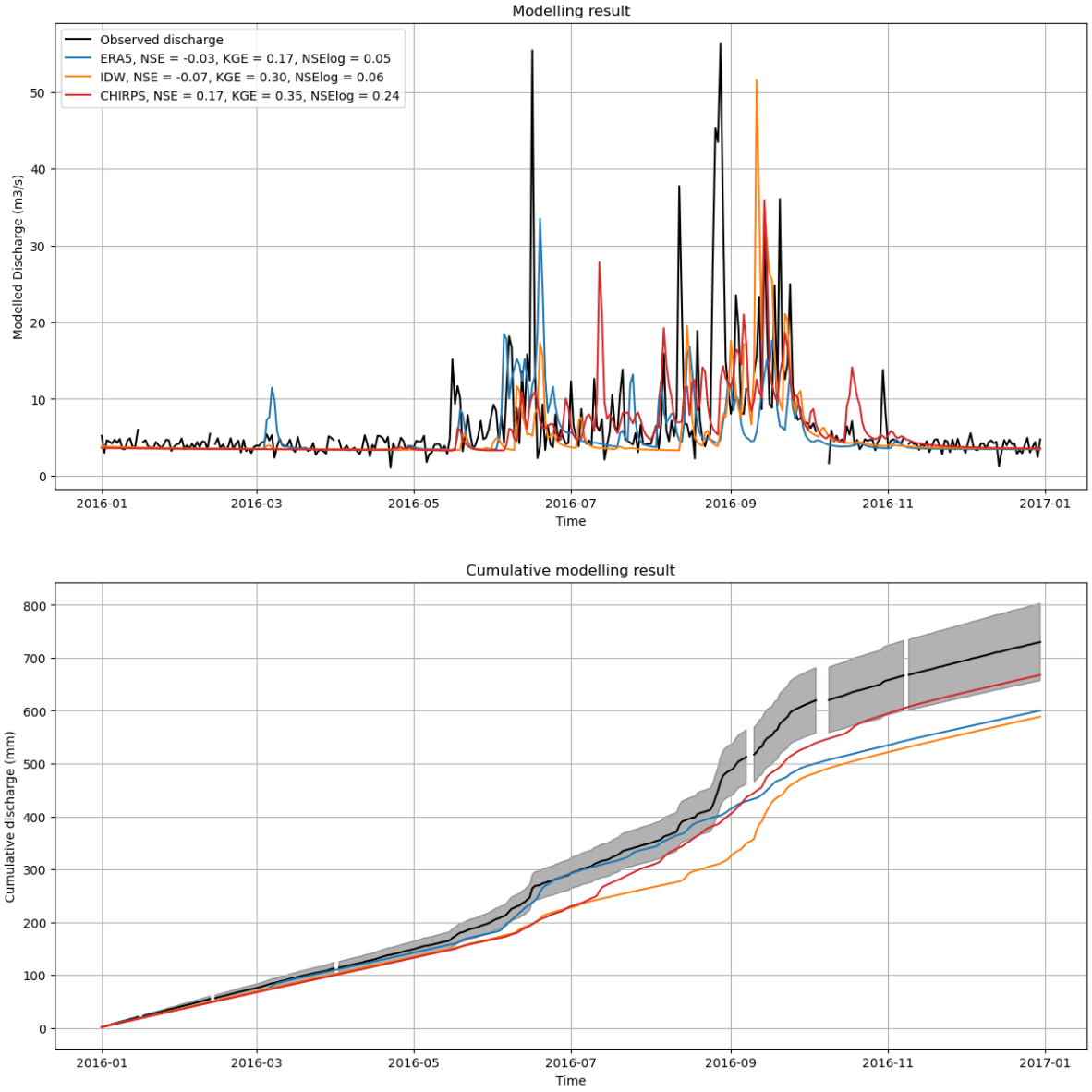

Figure A.4: Model run 2016

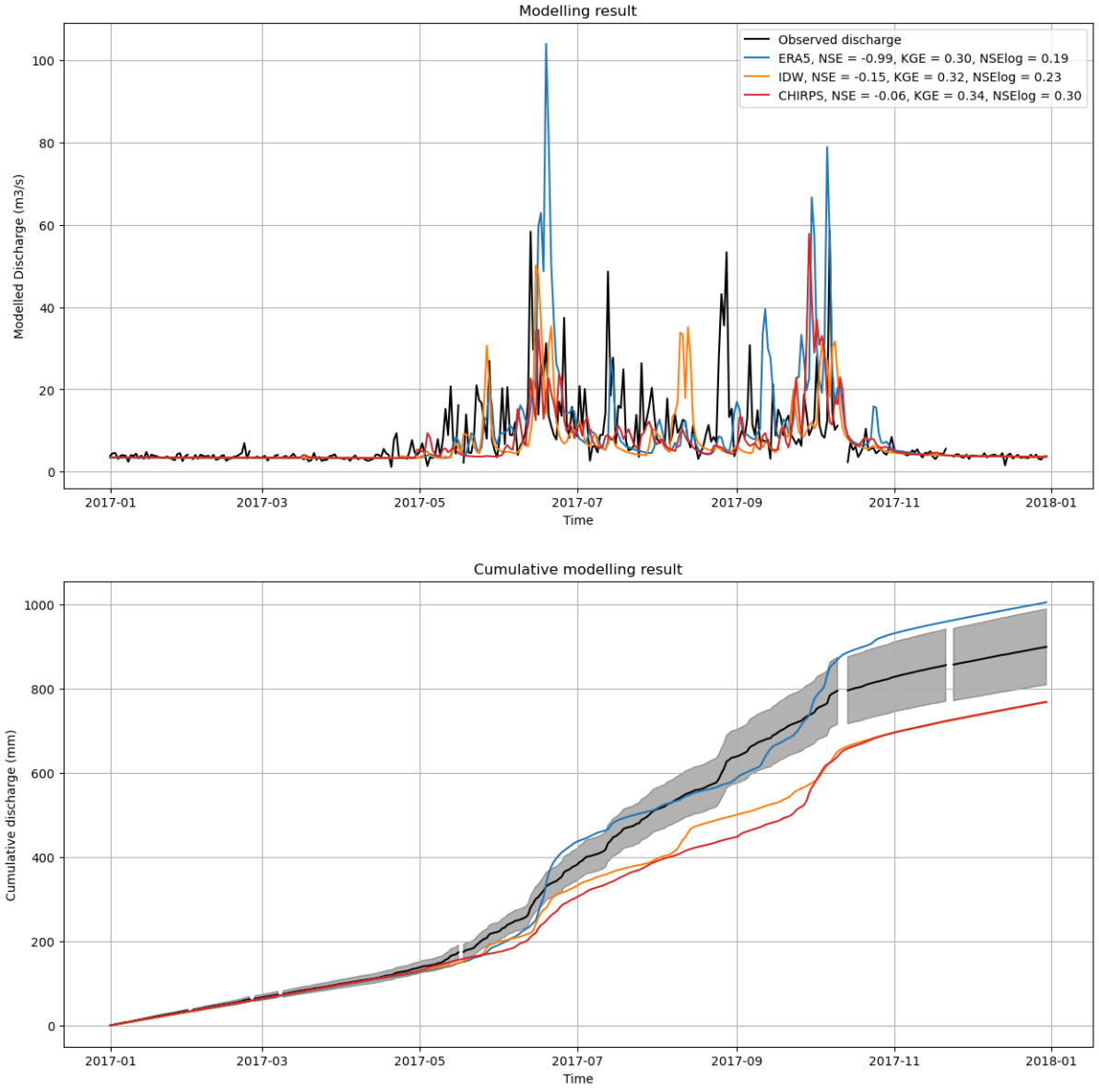

Figure A.5: Model run 2017

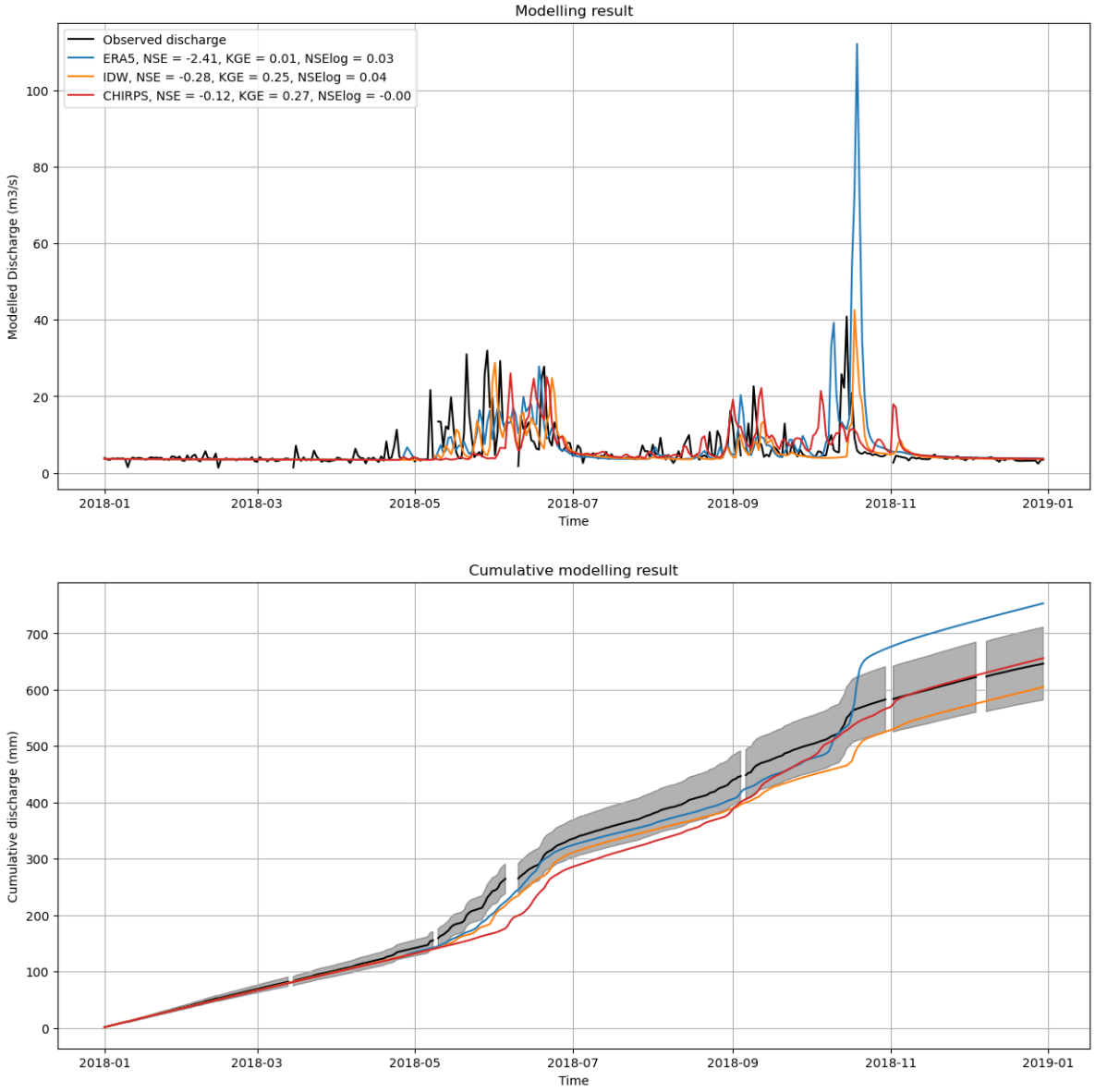

Figure A.6: Model run 2018

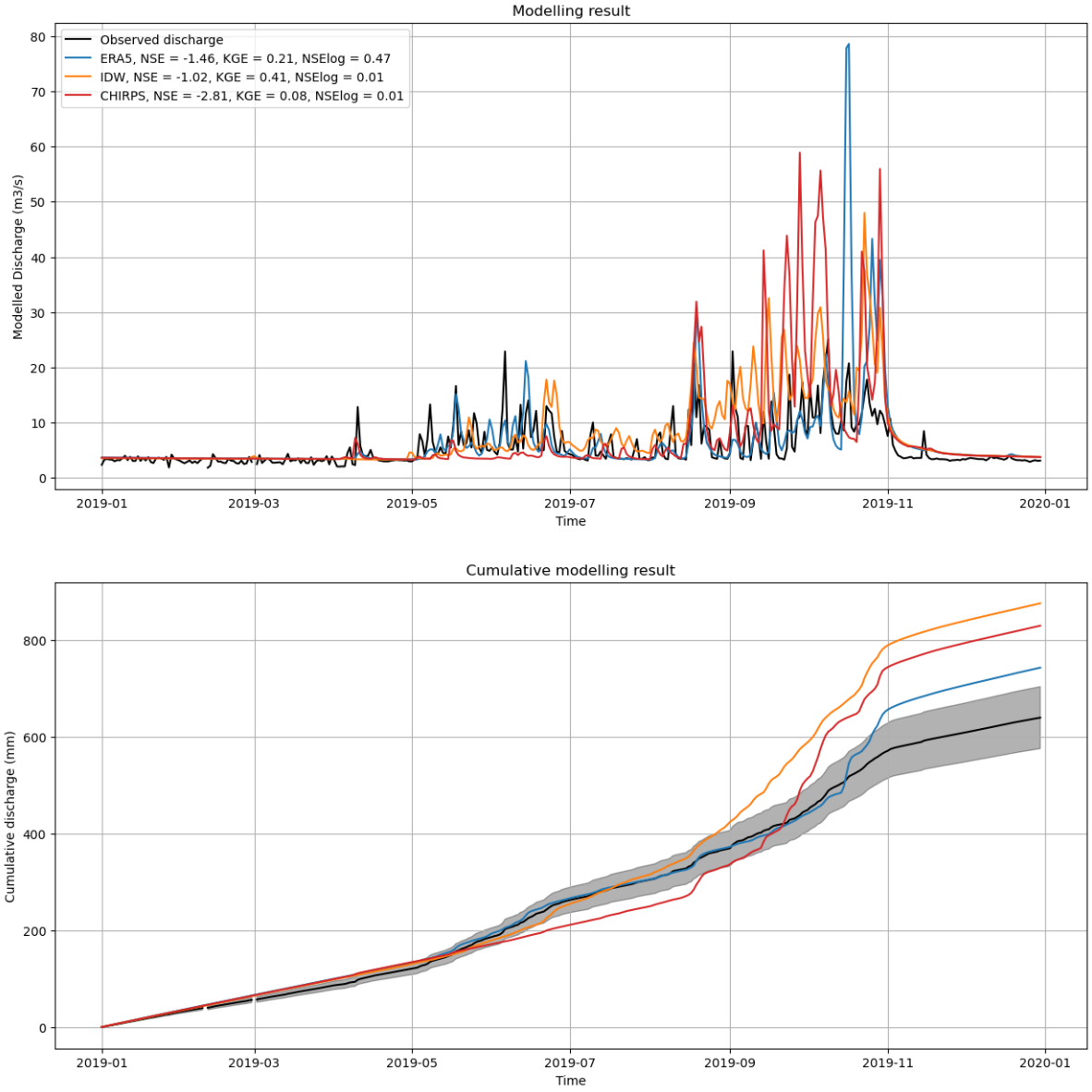

Figure A.7: Model run 2019